



Universidad Autónoma  
de Madrid

**Biblos-e Archivo**  
Repositorio Institucional UAM

**Repositorio Institucional de la Universidad Autónoma de Madrid**

<https://repositorio.uam.es>

Esta es la **versión de autor** del artículo publicado en:  
This is an **author produced version** of a paper published in:

Inorganic Chemistry 59.19 (2020): 13845-13857

**DOI:** <https://doi.org/10.1021/acs.inorgchem.0c01326>

**Copyright:** © 2020 American Chemical Society

El acceso a la versión del editor puede requerir la suscripción del recurso

Access to the published version may require subscription

# Photocatalytic Water Soluble Cationic Platinum(II) Complexes bearing Quinolate and Phosphine Ligands

*Pablo Domingo-Legarda,<sup>‡</sup> Antonio Casado-Sánchez,<sup>†</sup> Leyre Marzo,<sup>†</sup> José Alemán<sup>\*†§</sup> and Silvia Cabrera,<sup>\*‡§</sup>*

<sup>‡</sup> Inorganic Chemistry Department, Universidad Autónoma de Madrid, 28049 Madrid (Spain)

<sup>†</sup> Organic Chemistry Department, Universidad Autónoma de Madrid, 28049 Madrid (Spain).

<sup>§</sup> Institute for Advanced Research in Chemical Sciences (IAdChem), Universidad Autónoma de Madrid, 28049 Madrid (Spain).

ABSTRACT. Cationic Pt(II) complexes ([Pt(QO/S)(P<sup>^</sup>P)]X), having 8-oxy or 8-thioquinolate (QO/S) and seven different mono or bidentate phosphines as ligands, have been synthesized and characterized. The photophysical, stability and photocatalytic properties of those complexes were studied and compared to that of the parent [Pt(QO/S)(dmsO)(Cl)]. The coordination of phosphines induced a red-shift in the absorption energy of the MLCT band, whereas the emission wavelength

of the complexes only depended on the nature of the quinolate ligand. Moreover, the photocatalytic activity of the Pt(II) complexes was evaluated in the oxidation of sulfides using atmospheric oxygen as oxidant. All the complexes were active photocatalysts for that transformation, exhibiting [Pt(QO)(BINAP)]Cl and [Pt(QO)(SEGPPOS)]Cl (BINAP: 2,2'-bis(diphenylphosphino)-1,1'-binaphthyl, SEGPPOS: (4,4'-bi-benzodioxole)-5,5'-diylidiphosphine) high catalytic performance and stability. In addition, the enhanced water solubility of the complexes allowed to perform the photooxidation reaction under environmental friendly conditions. In particular, the catalyst [Pt(QS)(dppe)]Cl, bearing 8-thioquinolate and diphenylphosphinoethate (dppe) as ligands, successfully catalyzed the oxidation of a variety of sulfides using water as solvent.

## INTRODUCTION

The rich photochemical and photophysical properties of Pt(II) complexes have been extensively studied due to their wide applications in different areas, such as, organic light-emitting devices,<sup>1</sup> biosensors, probes and photosensitizers.<sup>2,3</sup> All those studies show that the luminescence of square-planar Pt(II) complexes can be ascribed to different nature, that are, metal-centered, metal-to-ligand, ligand centered, or arising from aggregates states. Moreover, heteroleptic complexes are the most studied because the ancillary ligand allows to easily tune the photophysical properties of the complexes. Consequently, for non-emissive complexes, the exchange of the ancillary ligand is a straightforward method to increase their emission properties. In this sense, it is well-known that strong field or multidentate ligands are the most appropriate ligands for raising the energy of the d-d state or suppressing excited state structural distortions, which are the main causes of non-radiative decay processes.

In the last years, photocatalysis has emerged as a powerful tool in organic synthesis to provide a great variety of transformations under mild reaction conditions.<sup>4</sup> The vast majority of examples are conducted using ruthenium(II) and iridium(III) complexes as catalysts, or organic molecules to a lesser extent. By contrast, the extensive knowledge in photophysical properties of platinum(II) complexes has been scarcely applied for the development of platinum(II)-based photocatalysts.<sup>5</sup> In this area, we developed a new family of platinum(II) photocatalysts formed by coordination of 8-oxyquinolate or 8-thioquinolate bidentate ligand, dimethylsulfoxide and a choride.<sup>6</sup> The design of those Pt(II) complexes was based on the luminescent properties reported for other 8-oxy- or 8-thioquinolate-metal complexes.<sup>7,8</sup> It is remarkable that those Pt(II) complexes are very easily prepared in one-step, starting from commercial available reagents, and do not require Schlenk techniques.<sup>9</sup> In addition, the complexes have proved to be efficient photocatalysts in the oxidation of sulfides<sup>6a</sup> along with other photoredox processes such as the cross-dehydrogenative-coupling, the asymmetric alkylation of aldehydes and the photooxidation of arylboronic acids.<sup>6b</sup> Despite the good photocatalytic performance of those complexes, their photophysical properties are far from optimal and their main drawbacks are related to the low luminescence and solubility. As aforementioned, ancillary ligands could play a key role in the emission of metallic complexes, as well as in solubility properties. For this reason, we envisage that the exchange of the chlorine and dimethylsulfoxide ligands of our family of platinum(II) complexes by mono- or bidentate phosphines will impose rigidity to the complex, and therefore their luminescence and photophysical properties will be improved. As reported in the literature, metallic complexes with phosphine ligands exhibit high luminescence due to the strong field ligand nature of phosphines, affecting the wavelength and lifetime of the emission state as well.<sup>10</sup> On the other hand, the quinolate-platinum(II) complexes are usually very planar structures, which could undergo

aggregation processes in solution that reduce their catalytic activity. On account of this, the binding of phosphines to the complexes would suppress aggregation due to the steric hindrance of the phosphine ligand. In addition to the above-commented advantages, we expect that the new designed Pt(II) complexes would be more soluble due to their cationic nature.

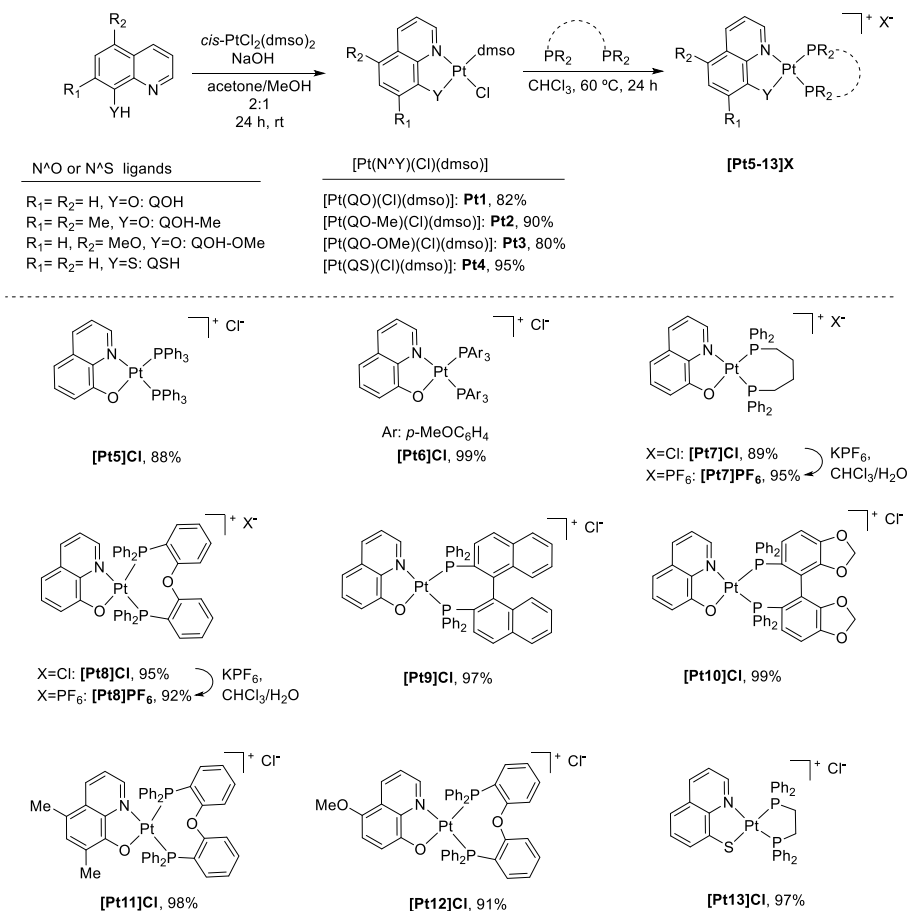
Herein, we present the synthesis, characterization and structural features of new cationic platinum(II) complexes bearing bidentate 8-hydroxy or 8-thiolquinolines and phosphine ligands. Phosphines of different electronic properties, coordination modes and bite angles were used to study their influence into the photophysical properties and catalytic activity of the complexes, comparing the results with those of the parent complex without phosphine. In addition, their catalytic performance was studied in the photooxidation of sulfides, allowing the reaction even in green solvents as water due to the good solubility of these cationic complexes in this media.

## RESULTS AND DISCUSSION

**Synthesis and Characterization of the  $[\text{Pt}(\text{QO/S})(\text{P}^{\wedge}\text{P})]\text{X}$ .** The cationic Pt(II) complexes **Pt5-13** were easily prepared in two steps starting from  $[\text{Pt}(\text{Cl})_2(\text{dmsO})_2]$  (Scheme 1). In the first step, the complexation of the corresponding 8-hydroxyquinoline ligand (QOH, QOH-Me or QOH-OMe) or 8-thioquinoline ligand (QSH) to the platinum center was carried out following a synthetic procedure previously reported.<sup>6,9</sup> Next, the ancillary chloride and dmsO ligands of the Pt(II) complexes **Pt1-Pt4** were replaced by mono- or bidentate phosphines. Starting from  $[\text{Pt}(\text{QO})(\text{Cl})(\text{dmsO})]$  **Pt1** complex, triphenyl- and tris(*p*-methoxyphenyl)phosphines were used as monodentate ligands for the synthesis of cationic complexes **[Pt5]Cl**<sup>11</sup> and **[Pt6]Cl**, respectively. The use of bidentate phosphines as ancillary ligand allows to study the influence of the bite angle, structural rigidity and electronic properties of the phosphine into their luminescence and catalytic

activity. For this purpose, bis(diphenylphosphino)ethane (dppe), bis(diphenylphosphinobutane (dppb), bis[(2-diphenylphosphino)phenyl]ether (DPEphos), 2,2'-bis(diphenylphosphino)-1,1'-binaphthyl (BINAP) and (4,4'-bi-benzodioxole)-5,5'-diylidiphosphine (SEGPPOS) were selected as ligands. The substitution reaction was carried out in refluxing chloroform for 18 h, leading to the corresponding chloride salts. Under those conditions, the dppb, DPEphos, BINAP and SEGPPOS coordination was successfully achieved in high yields, while dppe, which afforded chelates with small bite angle (86 °), gave complex reaction mixtures. Moreover, complexes **[Pt11]Cl** and **[Pt12]Cl**, having different substituents at the quinoline ring and DPEphos as ligand, were also isolated in 98% and 91% yields, respectively. By contrast, the coordination of phosphines to obtained thioquinolate complex derivatives was challenging and only the synthesis of the dppe coordinated complex **[Pt13]Cl** was attained. In addition, to study the influence of the counteranion in the catalytic performance of the complexes, the hexafluorophosphates salts of **[Pt7]<sup>+</sup>** and **[Pt8]<sup>+</sup>** were prepared by anion metathesis using KPF<sub>6</sub> in a mixture of chloroform and water as solvent.

**Scheme 1.** Synthesis of complexes [Pt(QO/S)(P<sup>^</sup>P)]X



All the complexes were characterized by <sup>1</sup>H, <sup>13</sup>C, <sup>195</sup>Pt and <sup>31</sup>P NMR experiments. Among them, the most relevant information was obtained from the spectra of <sup>195</sup>Pt and <sup>31</sup>P nucleus (Table 1). Regarding <sup>195</sup>Pt signals, all the (P<sup>^</sup>P)Pt complexes exhibited chemical shifts between -4035.2 and -4569.4 ppm, which corresponds to a significant upfield shift of the <sup>195</sup>Pt signal displacement of ~1200 ppm compared to their corresponding parent **Pt1-Pt4** complex. This shift together with the apparition of characteristic doublets arising from the <sup>31</sup>P-<sup>195</sup>Pt heterocoupling confirmed that the

phosphines are bonded to the Pt center. On the other hand, in the  $^{31}\text{P}$  NMR spectra, two chemical shifts flanked by platinum satellites can be ascribed to the inequivalent P atoms of the complexes. In addition, the small P–P coupling ( $J_{\text{Pa,Pb}} = 8.9\text{--}30.1$  Hz) confirmed the *cis* disposition of the two phosphorus atoms and their coupling through the platinum center. In the case of the anionic complexes with  $\text{PF}_6^-$  as counteranion, the spectra also exhibited an extra heptet signal at  $-144$  ppm. The analysis of the  $^{31}\text{P}$  NMR data of all the complexes showed some trends in the phosphorous chemical shifts and the Pt–P coupling constants (Table 1). For the 8-oxyquinolate complexes, the P atom in *trans* position with respect to the phenolate ( $\text{P}_a$ ) is less shielded than the P atom *trans* to the N of the quinoline ring ( $\text{P}_b$ ). In addition, the increase in the electron density of the phosphine led to a more shielded chemical shifts in both phosphines (compare complexes **[Pt5]** with **[Pt6]** and **[Pt7]** in Table 1). By contrast, the electron-rich methyl and methoxy substituents at the 8-oxyquinolate ligand did not produce any significant displacement in the phosphorous chemical shifts. Regarding complex **[Pt13]**, the  $^{31}\text{P}$  signals were notably shifted towards the downfield region due to the binding of the 8-thioquinolate ligand, which was also observed in the  $^{195}\text{Pt}$  NMR spectra. It is also reported that the Pt–P coupling constant depends on the *trans* influence of the ligand in *trans* position respect to the P, the nature of the phosphine and the size of the chelate formed after coordination.<sup>12</sup> The analysis of the coupling constants obtained together with the structure of the complexes led to some trends. Firstly, the low  $J_{\text{Pt-Pa}}$  values of complex **[Pt13]** could be ascribed to the higher *trans* influence of the S atom of the quinolate ligand in comparison with the N atom and the small size of the dppe-chelate ring. In addition, for the 8-oxyquinolate complexes, the higher Pt– $\text{P}_a$  coupling constant showed the lower *trans* influence of the phenolate fragment compared to the pyridine fragment of the ligand, which was also in agreement with the Pt–P distance found in the X-ray structures (see below). It is also important to notice the



upshielding of the P signals in the DPEphos coordinated complexes (see **[Pt8]**, **[Pt11]** and **[Pt12]**) together with an increase in the Pt-P coupling constant values, being the P in *trans* position respect to the N affected to a greater extent. This fact could be attributed to the higher steric hindrance imposed by the DPEphos ligand.

**Table 1.** Relevant  $^{195}\text{Pt}$  and  $^{31}\text{P}$  NMR data for selected complexes.<sup>a</sup>

Complex	$\delta$ Pt (ppm)	$J_{\text{Pt,P}_a}$ (Hz)	$J_{\text{Pt,P}_b}$ (Hz)	$\delta$ P <sub>a</sub> (ppm)	$\delta$ P <sub>b</sub> (ppm)	$J_{\text{P}_a,\text{P}_b}$ (Hz)
<b>[Pt5]Cl</b>	-4210.3	3672.5	3394.3	14.1	8.7	25.0
<b>[Pt6]Cl</b>	-4211.0	3693.9	3423.0	10.7	4.9	24.6
<b>[Pt7]Cl</b>	-4264.4	3432.9	3315.7	9.5	4.2	29.0
<b>[Pt8]Cl</b>	-4154.0	3553.1	3716.6	2.5	-1.3	24.3
<b>[Pt9]Cl</b>	-4035.2	3583.5	3415.7	6.5	5.1	29.9
<b>[Pt10]Cl</b>	-4089.2	3561.1	3435.1	4.0	3.5	30.1
<b>[Pt11]Cl</b>	-4149.2	3531.1	3688.5	3.1	-1.3	24.8
<b>[Pt12]Cl</b>	-4136.4	3521.0	3733.0	2.6	-1.2	24.4
<b>[Pt13]Cl</b>	-4569.4	2864.1	3216.1	51.3	36.8	8.9

<sup>a</sup> Data acquired at 64.5 MHz for  $^{31}\text{P}$  and 122 MHz for  $^{195}\text{Pt}$  in  $\text{CDCl}_3$  as solvent. P<sub>a</sub> denotes the P *trans* respect to the O or S atoms. P<sub>b</sub> denotes the P atom *trans* respect to the N atom.

The slow evaporation of chloroform solutions of complexes **[Pt6]Cl**, **[Pt7]PF<sub>6</sub>**, **[Pt8]Cl**, **[Pt9]PF<sub>6</sub>** and **[Pt13]Cl** afforded single crystals suitable for X-ray diffraction analysis (Figure 1).<sup>13</sup> Table 2 outlines the most important structural features regarding bond lengths and angles of the crystallographic data of those Pt complexes. First, all the complexes exhibit a distorted square-planar geometry, in which the angle O(1)-Pt(1)-N(1) or S(1)-Pt(1)-N(1) is close to 80° due to the restrictions imposed by the chelation of 8-oxy- or 8-thioquinolate ligand. In addition, the coordination of dppb, BINAP and tris(*p*-methoxyphenyl)phosphine induce the slightly deviation of one of the phosphorous donor atom from the coordination plane, which is formed by Pt(1), N(1),

O(1), P(1) and P(2). In those complexes, there is also a 10-20° deviation between the 8-oxyquinolate ring and the coordination plane. On the contrary, the 8-thioquinolate complex **[Pt13]Cl** shows a perfectly planar disposition, being the aromatic ligand and the metalated ring in the same plane. Regarding bond distances, the Pt-O and Pt-N bond of **[Pt6]Cl**, **[Pt7]PF<sub>6</sub>**, **[Pt8]Cl** and **[Pt9]PF<sub>6</sub>** are slightly longer than that of the previously described [Pt(N<sup>^</sup>O)(Cl)(dmsu)] complex<sup>9</sup> due to the strong trans influence of the phosphine ligands. In addition, the two Pt-P distances are different in each complex. For the complexes bearing bidentate phosphines, the distance of Pt-P bond *trans* to oxygen are shorter than the Pt-P bond distance *trans* to nitrogen. This observation suggests the higher trans influence of the pyridine ring and is in agreement with the trend observed in the  $J_{Pt,P}$  values. It is also important to notice that although DPEphos can potentially display  $\kappa^1$ -,  $\kappa^2$ - or  $\kappa^3$ -binding modes,<sup>14</sup> the solid structure of **[Pt8]Cl** shows a  $\kappa^2$ -P,P-bidentate coordination mode of that ligand in the complex.

The bite P-Pt-P angles of complexes **[Pt7]PF<sub>6</sub>**, **[Pt8]Cl**, **[Pt9]PF<sub>6</sub>** and **[Pt13]Cl**, with coordinated bidentate phosphines, are comparable to those previously reported.<sup>15</sup> In this regard, for those complexes bearing 8-oxyquinolate and bidentate phosphines (**[Pt7]PF<sub>6</sub>**, **[Pt8]Cl** and **[Pt9]PF<sub>6</sub>**) the bite angle size of the phosphine plays an important role into the Pt-P bond lengths, instead of the electron-acceptor character of the phosphine. On account of this, the longer Pt-P bonds (2.287 and 2.252 Å) are found in the DPEphos coordinated complex **[Pt8]Cl**, which has the greatest bite angle (96.51°). Further analysis of the crystal structure of the thiolate complex **[Pt13]Cl** reveals the presence of a  $\pi$ - $\pi$  interaction (3.357 Å) between the pyridine ring of one complex and the aromatic ring of the phosphine of another platinum complex molecule. The other complexes do not present  $\pi$ - $\pi$  or metal-metal interaction between molecules.

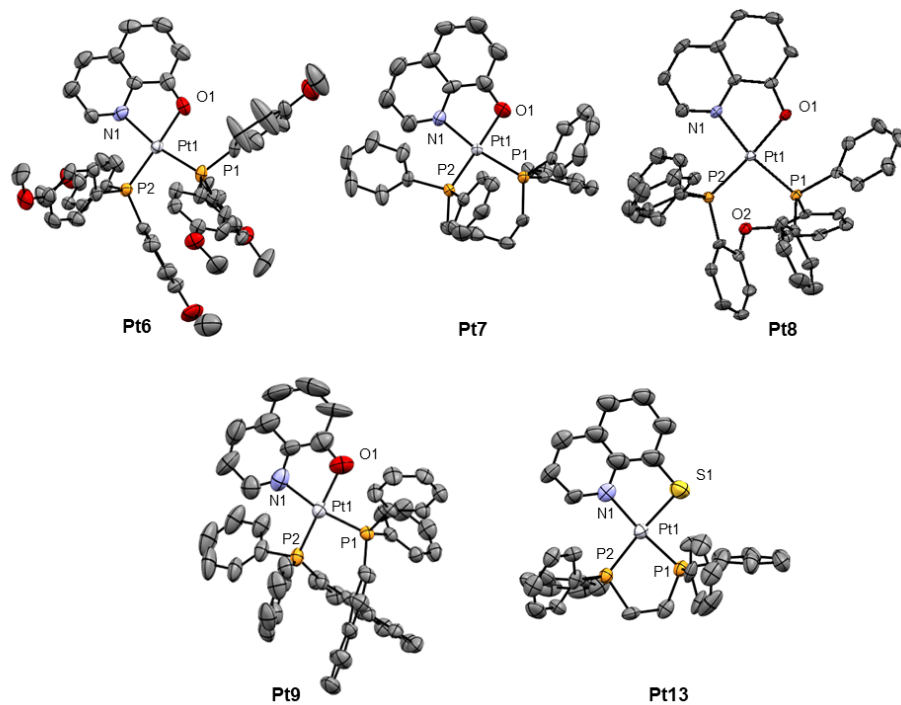


**Figure 1.** ORTEP view of complexes **Pt6-Pt9** and **Pt13**. Hydrogen bonds, counteranions and solvent molecules are omitted for clarity. Thermal ellipsoids are shown at the 50% probability level.

**Table 2.** Selected bond lengths (Å) and angles (°) for Pt(II) complexes.

Bond lengths	[Pt6]Cl	[Pt7]PF <sub>6</sub>	[Pt8]Cl·4CHCl <sub>3</sub>	[Pt9]PF <sub>6</sub> ·CHCl <sub>3</sub>	[Pt13]Cl
Pt(1)-N(1)	2.109(8)	2.082(5)	2.120(6)	2.113(7)	2.110(2)
Pt(1)-O(1)	2.067(6)	2.054(4)	2.024(5)	2.091(6)	-
Pt(1)-P(1)	2.260(2)	2.256(1)	2.287(2)	2.250(2)	2.231(7)
Pt(1)-P(2)	2.271(2)	2.247(1)	2.252(2)	2.240(2)	2.272(7)
Pt(1)-S(1)	-	-	-	-	2.305(8)
Angles	[Pt6]Cl	[Pt7]PF <sub>6</sub>	[Pt8]Cl·4CHCl <sub>3</sub>	[Pt9]PF <sub>6</sub> ·CHCl <sub>3</sub>	[Pt13]Cl

O(1)-Pt(1)-N(1)	80.7(3)	80.1(2)	80.2(2)	79.3(3)	-
O(1)-Pt(1)-P(1)	88.0(2)	88.02(1)	88.4(2)	89.3(2)	-
S(1)-Pt(1)-N(1)	-	-	-	-	83.5(6)
S(1)-Pt(1)-P(1)	-	-	-	-	89.6(3)
N(1)-Pt(1)-P(2)	96.1(2)	99.9(1)	94.9(2)	101.6(2)	101.7(6)
P(1)-Pt(1)-P(2)	95.9(9)	92.7(5)	96.5(7)	91.6(5)	85.3(3)

**Absorption and photoluminescence spectra.** Absorption and emission spectra at different temperatures, as well as quantum yields and emission lifetimes, were recorded for all the complexes. The most important data are listed in Table 3. Firstly, the UV-Vis spectra of all the platinum complexes in EtOH solution showed two different regions that were assigned by comparison with those of [Pt(QO)(Cl)(dmsO)] (**Pt1**) and [Pt(QS)(Cl)(dmsO)] (**Pt4**).<sup>6</sup> The higher energy region (226-274 nm) contained the more intense absorption bands, which are characteristic of the  $\pi$ - $\pi^*$  ligand-centered transitions of both the quinoline and phosphine ligands. On other hand, low energy transitions between 420 and 476 nm (extinction coefficients in the range 2033-3962 L·mol<sup>-1</sup>·cm<sup>-1</sup>) are ascribed to metal-to-ligand charge transfer (MLCT) bands between the HOMO orbital (centered at the metal) and the LUMO orbital (centered at the QO/QS ligand). Generally, the binding of the phosphine to the complex leads to a red-shift of ~20 nm in the maximum of the MLCT wavelength band, regardless of the nature of the phosphine. In addition, the energy of the MLCT band of the complexes is independent of the coordinated phosphine ligand and the counteranion. As an illustrative example, Figure 2A shows the MLCT band of complexes containing PPh<sub>3</sub> (**Pt5**Cl), dppb (**Pt7**Cl) or DPEphos (**Pt8**Cl) as ligands, which are centered at 422 nm. However, there is a major dependence of that band on the substitution at the ring of the quinoline ligand or the donor atom (oxygen vs sulfur). Therefore, the incorporation of electron-rich substituents at the aromatic ring of the quinolate ligand gives a bathochromic shift in the

MLCT band (Figure 2B). The group of Zhao<sup>16</sup> has previously reported that the addition of electron donating groups at the quinoline increases the contribution of the p orbital of the oxygen/sulfur atom of the ligand into the HOMO orbital, raising its energy, whereas the LUMO orbital energy remains unaltered. In summary, the energy of the MLCT absorption band of these Pt complexes can be tuned by the electronic nature of the substituents at the aromatic quinoline or the S/O donor atom, without a significant contribution of the phosphine ligands.

Upon irradiation at the MLCT band, complexes **Pt1**-**[Pt13]** exhibited low luminescence in EtOH solution at 298 K with very short lifetimes ( $< 10$  ns) and low luminescence quantum yields in most of the cases. In general, the emission spectra of all the complexes display two bands between 488 and 551 nm. It is important to notice that the emission wavelengths are slightly influenced by the nature of the quinolate ligand, whereas the effect of the phosphine is negligible. In addition, for all complexes, the wavelength and shape of the emission bands are independent of the excitation wavelength, and the emission spectra do not depend on the complex concentration, excluding emission phenomena from complex aggregation. Importantly, the coordination of triphenylphosphines (**[Pt5]Cl**) and dppe (**[Pt13]Cl**) produces an important increased in the emission efficiency. However, a plausible explanation of such effect cannot be given due to the absence of a relationship between the steric and electronic properties of the phosphines and the quantum yields observed. Finally, the nature of the anion does not affect the wavelength of the emission band nor the quantum efficiencies or lifetimes (see SI).

On the other hand, higher emissions were recorded in glassy ethanolic solutions at 77 K. Furthermore, the energy of the emission bands is almost the same than those recorded at room temperature, yet for some complexes, an additional band at  $\sim 610$  nm appeared.

**Table 3.** UV-Vis absorption and emission data for complexes **Pt1-Pt13**.<sup>a</sup>

Complex	Absorption, 298 K <sup>b</sup>			Emission, 298 K <sup>c</sup>			Emission, 77 K <sup>c</sup>
	$\lambda_{\text{abs}}/\text{nm}$ ( $\epsilon/\text{L}\cdot\text{mol}^{-1}\cdot\text{cm}^{-1}$ )			$\lambda_{\text{em}}/\text{nm}$	$\phi_{\text{PL}}$ (%)	$\tau$ (ns)	$\lambda_{\text{em}}/\text{nm}$
<b>Pt1</b>	236	(12645),	266	494, 532	0.01	< 2	581
	(19946), 403 (2535)						
<b>Pt2</b>	208	(12617),	272 (8817),	485, 529	0.01	< 2	480, 530
	434 (1250)						
<b>Pt3</b>	272	(17773),	353 (2215),	508, 551	0.04	< 2	537, 553
	452 (2698)						
<b>[Pt5]Cl</b>	267	(22650),	422 (2500)	493, 538	0.21	< 2	493, 528, 607
<b>[Pt6]Cl</b>	249	(72863),	427 (3871)	493, 534	0.07	< 2	493, 524, 614
<b>[Pt7]Cl</b>	236	(41395),	267	499, 536	0.09	< 2	489, 531, 611
	(18671), 422 (2529)						
<b>[Pt8]Cl</b>	237	(40660),	265	494, 532	0.01	< 2	492, 527, 619
	(22822), 427 (2888)						
<b>[Pt9]Cl</b>	237	(79345),	265	493, 536	0.02	6	490, 529, 610
	(39685), 429 (4872)						
<b>[Pt10]Cl</b>	267	(25415),	316,	493, 533	0.02	< 2	491, 533, 613
	(12613), 423 (3962)						
<b>[Pt11]Cl</b>	273	(23779),	456 (3536)	493, 540	0.01	10	496, 542
<b>[Pt12]Cl</b>	248	(38159),	274	564	0.03	4	539, 576
	(23171), 476 (2033)						
<b>[Pt13]Cl</b>	256	(28152),	441 (3282)	536	0.12	< 2	497, 531, 619

<sup>a</sup> Due to the insolubility of complex **Pt4** in EtOH, its photophysical data was not obtained. <sup>b</sup> UV/Vis absorption measured in EtOH solution (see S.I for more details). <sup>c</sup> Emissions recorded at  $\lambda_{\text{exc}}$ = 403-476 nm in EtOH solution.

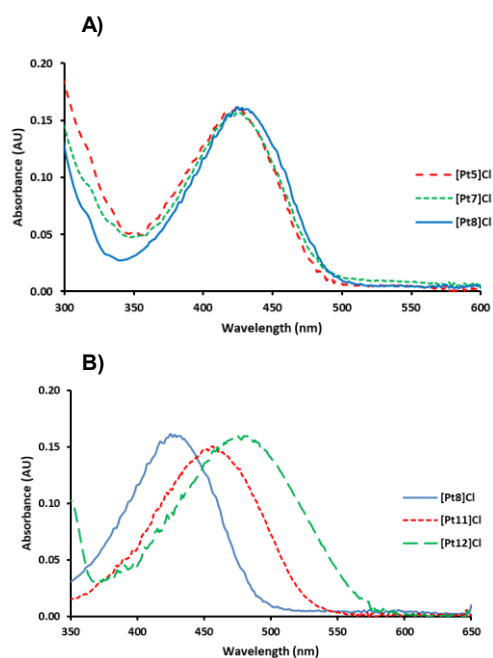


**Figure 2.** A) Phosphine effect: UV-Vis spectra of complexes **[Pt5]Cl**, **[Pt7]Cl** and **[Pt8]Cl** at  $10^{-4}$  M in EtOH. B) Quinolinate effect: UV-Vis spectra of complexes **[Pt8]Cl**, **[Pt11]Cl** and **[Pt12]Cl**, at  $10^{-4}$  M in EtOH.

**Electrochemistry.** First, the redox potentials of the complexes were determined by cyclic voltammetry (CV) in deaerated acetonitrile as solvent. All the complexes underwent an irreversible oxidation in the range 1.12-1.38 V and an irreversible reduction between -0.76 and -1.44 V. The irreversible nature of the redox processes of these Pt(II) complexes is in accordance to the fact that those species can undergo nucleophilic attack by solvents, as previously reported for other Pt(II) complexes.<sup>17</sup> Regarding the complexes bearing the quinolinate (QO) ligand (**Pt1**, **[Pt5-10]Cl**), there is not a clear trend between the oxidation or reduction values of the complexes and the electron-donating ability of the coordinated phosphine. However, the coordination of monodentate

or bidentate phosphines shifts the oxidation peaks to lower values, being this process more favorable than that of the parent **Pt1** complex. By contrast, complex **[Pt13]Cl**, with dppe coordinated, is less prone to oxidation but more to reduction than **Pt4**.

The estimation of the excited state redox potential of the complexes was calculated from the ground state redox potentials of the complexes and the singlet state energy ( $E_{0-0}$ ) as mentioned in Table 4. The calculated excited state redox values have shown that the complexes **Pt5-Pt13**, having phosphine ligands, can act as strong oxidants or reductants, being the strongest oxidant complex **[Pt13]Cl** while the strongest reductant is **[Pt5]Cl**.

**Table 4.** Ground and excited state redox potential for selected Pt(II) complexes.<sup>a</sup>

Complex	$E_{ox}^p$ (V)	$E_{red}^p$ (V)	$E_{0-0}$ (eV) <sup>b</sup>	$E_{ox}^*$ (V) <sup>c</sup>	$E_{red}^*$ (V) <sup>c</sup>
<b>Pt1</b>	1.63	-1.38	2.87	-1.24	1.49
<b>Pt4</b>	1.29	-1.30	2.46	-1.17	1.16
<b>[Pt5]Cl</b>	1.12	-1.32	2.63	-1.51	1.31
<b>[Pt6]Cl</b>	1.38	-1.36	2.65	-1.27	1.29
<b>[Pt7]Cl</b>	1.28	-1.44	2.66	-1.38	1.22
<b>[Pt8]Cl</b>	1.22	-1.28	2.60	-1.38	1.32
<b>[Pt9]Cl</b>	1.26	-1.36	2.61	-1.35	1.25
<b>[Pt10]Cl</b>	1.18	-1.43	2.65	-1.47	1.22
<b>[Pt13]Cl</b>	1.38	-0.76	2.54	-1.16	1.78

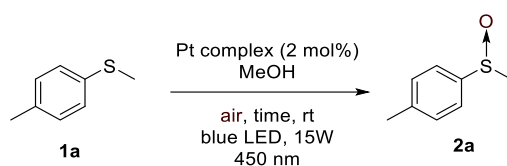
<sup>a</sup> Conditions: 20 mV·s<sup>-1</sup> scan rate; 1.0 mM solution of complex in argon-saturated CH<sub>3</sub>CN solution; 0.1 M solution of Bu<sub>4</sub>NPF<sub>6</sub>; glassy carbon disk (2.8 mm diameter) as working electrode; platinum wire as counter electrode; Ag/AgCl as reference electrode. <sup>b</sup> Singlet state energy determined from the intersection of the normalized absorbance and emission spectra and converted into eV. <sup>c</sup> Excited state redox potentials estimated using the equation:  $E_{ox}^* = E_{ox} - E_{0-0}$  or  $E_{red}^* = E_{red} + E_{0-0}$ .



**Photocatalytic activity of the [Pt(QO/S)(P<sup>^</sup>P)]X complexes.** The new cationic phosphine coordinated complexes were tested as photocatalysts in the photooxidation of sulfides using atmospheric oxygen as oxidant.<sup>18</sup> This transformation is of utmost importance because sulfoxides moieties are found in many drugs and natural products, and are also crucial in organic synthetic transformations.<sup>19</sup> The selection of that reaction is based on the successful photocatalytic activity of the former complexes **Pt1** and **Pt4**.<sup>6a</sup> The oxidations were carried out using methyl *p*-tolylsulfide (**1a**) as substrate, 2 mol% of the Pt complex in methanol as solvent, and the reactions were stirred in open vials under the irradiation of blue LEDs. For comparison purposes, complexes **Pt1** and **Pt4** were also evaluated under the same conditions and all the results are shown in Table 5. First, the former catalysts **Pt1** and **Pt4** fully oxidized sulfide **1a** into **2a** in 12 h (entries 1-2). Besides, the new phosphine coordinated complexes prepared **Pt5-Pt13** are able to oxidize sulfide **1a** as well. However, the nature of the phosphines notably influences the catalytic performance of the complex. Specifically, complexes containing triphenylphosphines (entry 3), and DPEphos (entries 7-8) as ligands are less prone to catalyze the oxidation of substrate **1a**, having for those complexes less than 93% of conversion at 24 h. Moreover, the couples [**Pt8**]**Cl** and [**Pt8**]**PF<sub>6</sub>** (entries 7-8) or [**Pt9**]**Cl** and [**Pt9**]**PF<sub>6</sub>** (entries 9-10) show similar reaction rates, which excludes a counteranion effect into the activity. On the other hand, the presence of electron-donor groups into the 8-oxyquinolate ligand ([**Pt11**]**Cl** and [**Pt12**]**Cl**) seems to be detrimental for the photooxidation process (see entries 12-13), being the less active complexes of the family. An analysis of the oxidation outcome at different reaction times indicates that complexes [**Pt7**]**Cl** and [**Pt13**]**Cl**, having both alkyl-diarylphosphines, are able to oxidize more than 90% of sulfide **1a** in only 6 h with TOF numbers of 7.5 and 8.3 h<sup>-1</sup>, respectively (entries 5 and 14). Finally, it is important to

mention that the reaction does not take place in the absence of light, oxygen or photocatalyst, indicating their key role in the reaction.

**Table 5.** Screening of Pt complexes **Pt1**, **Pt4-Pt13** for the photooxidation of methyl-*p*-tolylsulfide **1a**.<sup>a</sup>



Entry	Complex	Conversion (%) <sup>b</sup>			TOF (h <sup>-1</sup> ) <sup>c</sup>
		6 h	12 h	24 h	
1	<b>Pt1</b>	82	100	100	6.8 <sup>d</sup>
2	<b>Pt4</b>	-	70	100	2.9
3	<b>[Pt5]Cl</b>	-	29	55	1.2
4	<b>[Pt6]Cl</b>	-	69	100	2.9
5	<b>[Pt7]Cl</b>	90	100	100	7.5 <sup>d</sup>
6	<b>[Pt7]PF<sub>6</sub></b>	-	96	100	4.0
7	<b>[Pt8]Cl</b>	-	72	93	3.0
8	<b>[Pt8]PF<sub>6</sub></b>	-	68	91	2.8
9	<b>[Pt9]Cl</b>	-	88	100	3.7
10	<b>[Pt9]PF<sub>6</sub></b>	-	86	100	3.6
11	<b>[Pt10]Cl</b>	-	97	100	4.0
12	<b>[Pt11]Cl</b>	-	41	72	1.7
13	<b>[Pt12]Cl</b>	-	21	52	0.9
14	<b>[Pt13]Cl</b>	99	100	100	8.3 <sup>d</sup>

<sup>a</sup> Reaction conditions: Open vials containing **1a** (0.2 mmol) and 2 mol% of the corresponding Pt complex in 2 mL of MeOH were irradiated under blue LED for the indicated time. <sup>b</sup> Determined

by  $^1\text{H}$  NMR analysis of the crude mixture. <sup>c</sup> Turnover frequency estimated after 12 h of reaction time. <sup>d</sup> Turnover frequency estimated after 6 h of reaction time.

With the most active complexes (**[Pt6]Cl**, **[Pt7]Cl**, **[Pt9]Cl**, **[Pt10]Cl** and **[Pt13]Cl**) in hand, we decide to evaluate their robustness and their stability. To this aim, we performed an experiment in which a fixed amount of Pt complex was tested in different catalytic runs, adding consecutive amounts of sulfide **1a** every 24 h (Figure 3). The same essay was carried out with complexes **Pt1** and **Pt4** for comparison purposes. As shown in Figure 3, the photocatalytic activity of complexes **Pt1**, **Pt4**, **[Pt6]Cl** and **[Pt7]Cl** was stopped in the second addition of sulfide **1a**, being only formed 0.3-0.4 mmol of sulfoxide **2a** after 48 h. Surprisingly, complexes **[Pt9]Cl** and **[Pt10]Cl**, with BINAP or SEGPHOS ligands respectively, showed an outstanding catalytic outcome, which could be due to their higher stability under these photocatalytic conditions. In fact, both photocatalysts were able to performed five consecutive catalytic runs, forming 1 mmol of product **2a** (154.2 mg) using only 3.8 mg of either **[Pt9]Cl** or **[Pt10]Cl** complex. These experiments show the enhancement of the robustness of the complexes caused by the coordination of phosphine ligand.

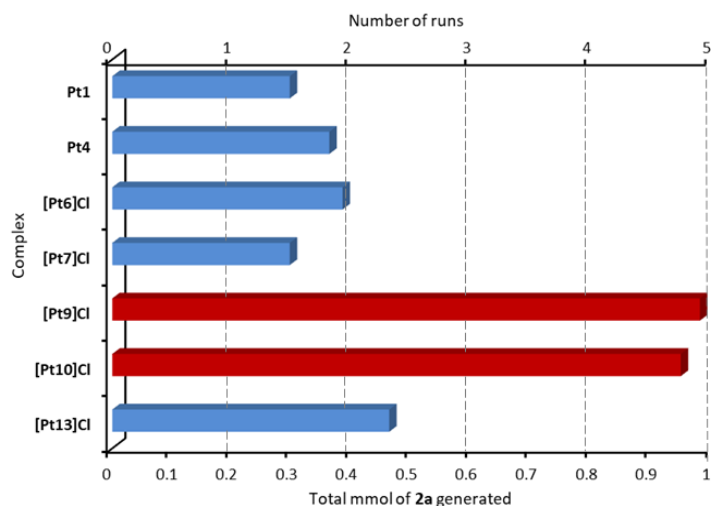


**Figure 3.** Total amount of sulfoxide **2a** (mmols) formed per 0.004 mmol of Pt complex. Those essays were performed by the addition of 0.20 mmol of sulfide **1a** to the reaction mixture every 24 h (each addition is a run). The final amount of sulfoxide **2a** produced was determined by NMR.

Another remarkable characteristic of the new cationic Pt complexes is their higher solubility compared to that of **Pt1** and **Pt4**, which might be one of the causes for their better catalytic performance. To analyze this property, the solubility value of the most active complexes in water and dichloromethane was determined following a established procedure (Table 6).<sup>20</sup> The less soluble complex in CH<sub>2</sub>Cl<sub>2</sub> is **Pt4**, which is in agreement with its low solubility in most of the solvents. This effect could be attributed to its planar structure and the strong interaction between molecules, that consequently reduces its applicability as catalyst in many solvents. Gratefully, the solubility of the coordinated dppe complex **[Pt13]Cl** resulted to be 29.0 mg·mL<sup>-1</sup>, representing a 32-fold increase over the poorly soluble compound **Pt4**. This remarkable effect was not observed for the cationic complexes based on **Pt1**. In those complexes, the highest solubility, that is 115.0

mg·mL<sup>-1</sup>, was obtained for the SEGPPOS-coordinated complex **[Pt10]Cl** (up to 5-fold respect to **Pt1**). Regarding the water solubility, the former **Pt1** and **Pt4** complexes were not fully stable in water and their solubility was not determined. By contrast, the cationic complexes **[Pt7]Cl**, **[Pt9]Cl**, **[Pt10]Cl** and **[Pt13]Cl** were perfectly stable and soluble in water, and their solubility values vary from 0.9 to 14.4 mg·mL<sup>-1</sup>. These results highlight the great improvement in the physical and chemical properties of the Pt complexes with respect to **Pt1** and **Pt4**, which is achieved by the coordination of phosphine ligands.

**Table 6.** Solubility data of Pt complexes in dichloromethane and water.<sup>a</sup>

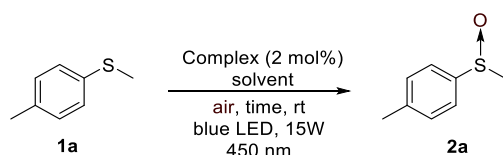
Complex	Solubility (mg·mL <sup>-1</sup> )	
	H <sub>2</sub> O	CH <sub>2</sub> Cl <sub>2</sub>
<b>Pt1</b>	- <sup>b</sup>	22.5 ± 0.7
<b>Pt4</b>	- <sup>b</sup>	0.9 ± 0.1
<b>[Pt7]Cl</b>	3.5 ± 0.3	59.2 ± 0.6
<b>[Pt9]Cl</b>	0.9 ± 0.1	22.0 ± 0.3
<b>[Pt10]Cl</b>	11.4 ± 0.1	115.0 ± 1.0
<b>[Pt13]Cl</b>	14.4 ± 0.1	29.0 ± 1.0

<sup>a</sup> Solubility determined by UV-Vis spectroscopy using standard curves.

<sup>b</sup> The complex was unstable in water solution. Standard deviations of at least 2 independent determinations.

The greater stability and solubility of the complexes encouraged us to study the possibility of carrying out the photooxidation of substrate **1a**, using greener solvents such as EtOH or even the less studied water.<sup>21</sup> Thus, we studied the photooxidation of **1a** using the most active cationic Pt complexes in water, or mixtures of EtOH:H<sub>2</sub>O as solvent (Table 7). Surprisingly, the oxidation of sulfide **1a** proceed in both solvent media with variable conversions, depending on the photocatalyst used. It is worth noting the good catalytic performance of complex **[Pt13]Cl**, which is able to fully oxidize substrate **1a** in pure water.

**Table 7.** Catalytic performance of Pt complexes in aqueous solutions for the photooxidation of *p*-methylphenylsulfide **1a**.<sup>a</sup>



Entry	Complex	Conversion (%) <sup>b</sup>	
		H <sub>2</sub> O:EtOH 3:1 (24 h)	H <sub>2</sub> O (48 h)
1	[Pt7]Cl	46	43
2	[Pt9]Cl	31	9 <sup>c</sup>
3	[Pt10]Cl	19	67
4	[Pt13]Cl	83	100

<sup>a</sup> Reaction conditions: Open vials containing **1a** (0.2 mmol) and 2 mol% of the corresponding Pt complex in 2 mL of the indicated solvent were irradiated under blue LED. <sup>b</sup> Determined by <sup>1</sup>H NMR analysis of the crude mixture. <sup>c</sup> The catalyst was not fully dissolved in the solvent.

The catalytic performance of [Pt13]Cl complex was further studied by, the oxidation of different sulfides using water as solvent (Figure 4). Under these photocatalytic conditions, alkylaryl sulfoxides **2a-2c** were isolated in moderate to good yields (48-97%), in which the steric hindrance imposed by the cyclopropyl substituent in the sulfide (**1c**) affected considerable the oxidation rate. In addition, the oxidation of dibutylsulfide **1d** was sluggish in water after 48 h, whereas 100% of yield of the methionine derivative **2e** was obtained. It is important to highlight that in all the cases the reaction was completely chemoselective, and the corresponding sulfoxide **2** was the only product obtained.

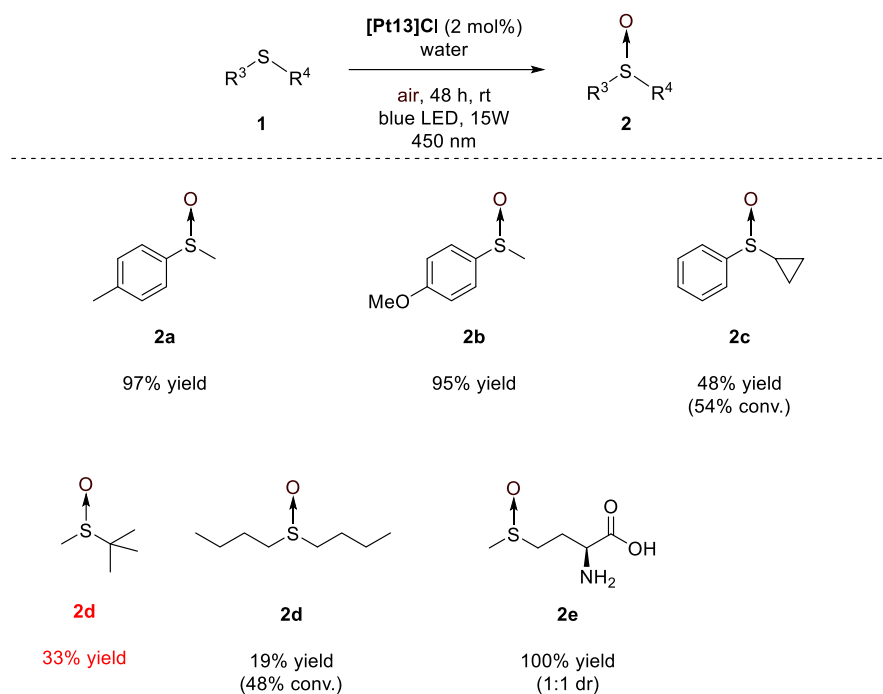


**Figure 4.** Scope of the photooxidation of sulfides **1** using **[Pt13]Cl** in water. Reaction conditions: Open vials containing sulfide **1** (0.2 mmol) and 2 mol% of **[Pt13]Cl** in 2 mL of water were irradiated under blue LED for 48 h. Isolated yield. Conversion determined by  $^1\text{H}$  NMR analysis of the crude mixture.

Finally, additional experiments support the photoredox pathway, via oxygen radical anion, as the most plausible mechanism for the photooxidation (see SI, Table S1). This data is in agreement with the mechanism previously reported by us for Pt(II) complexes.<sup>6a</sup>

## CONCLUSIONS

We have developed a new family of cationic Pt complexes ( $[\text{Pt}(\text{QO/S})(\text{P}^{\wedge}\text{P})]\text{X}$ ), having 8-oxy or 8-thioquinolate (QO/S) and seven different mono or bidentate phosphines as ligands. The coordination of the phosphine plays an important role in the photophysical, stability and photocatalytic properties of those complexes. The energy of the MLCT absorption band of these Pt complexes can be mainly tuned by the electronic nature of the substituents at the aromatic quinoline or the S/O donor atom. In addition, the coordination of phosphines induces a ca. 20 nm red-shift in the absorption wavelength, independently of the nature of the phosphine. Furthermore, the photocatalytic activity of these Pt complexes were studied in the photooxidation of sulfides to sulfoxides using atmospheric oxygen. The phosphine-coordinated complexes showed an enhance robustness and solubility in water, that allowed to successfully perform the photooxidation of different sulfides in a green solvent such as water.

## EXPERIMENTAL SECTION

**General methods and instrumentation.** Detailed information of the equipment and measures performed and general methods and materials are described in the Supporting Information.

**General procedure for the synthesis of complexes Pt1-Pt4.** To a solution of 22.4 mg of NaOH (0.56 mmol, 1.2 eq.) in 0.3 mL of MeOH, the corresponding quinoline ligand **QOH**, **QOH-Me**, **QOH-OMe** or **QSH** (0.55 mmol, 1.1 eq.) was added and the resulting suspension was stirred until the ligand was completely dissolved. Then, a suspension of 211.1 mg of *cis*- $\text{PtCl}_2(\text{dmsO})_2$ <sup>21</sup> (0.50 mmol, 1.0 eq.) in 0.6 mL of acetone was added and the reaction mixture was stirred at rt. After 24 h, the solid product was filtered, washed with cold water and ether, and dried under vacuum.



**Complex Pt1:**<sup>6,9</sup> Yellow solid (153.6 mg, 82 % yield). <sup>1</sup>H NMR (300 MHz, CDCl<sub>3</sub>): δ 9.38 (d, *J* = 4.6 Hz, 1H), 8.66 (d, *J* = 8.7 Hz, 1H), 7.70 (dd, *J* = 8.3, 4.9 Hz, 1H), 7.49 (t, *J* = 7.8 Hz, 1H), 7.17 (d, *J* = 7.9 Hz, 1H), 7.01 (d, *J* = 8.0 Hz, 1H), 3.61 (s, 6H).

**Complex Pt2:** Orange solid (181.2 mg, 90 % yield). <sup>1</sup>H NMR (300 MHz, CDCl<sub>3</sub>): δ 9.22 (d, *J* = 5.3 Hz, 1H), 8.27 (d, *J* = 8.4 Hz, 1H), 7.20 (s, 1H), 7.16 (dd, *J* = 8.4, 5.3 Hz, 1H), 3.66 (s, 6H), 2.55 (s, 3H), 2.50 (s, 3H). <sup>13</sup>C NMR (75 MHz, CDCl<sub>3</sub>): δ 162.0, 146.9, 143.6, 135.9, 133.2, 127.9, 125.3, 120.5, 119.0, 46.3, 16.9, 15.9. <sup>195</sup>Pt NMR (64.5 MHz, CDCl<sub>3</sub>): δ -2776.5. HRMS (ESI): calculated for C<sub>13</sub>H<sub>16</sub>ClNO<sub>2</sub>PtS, [M]<sup>+</sup> = 480.0289; found = 480.0280.

**Complex Pt3:** Red solid (161.9 mg, 80 % yield). <sup>1</sup>H NMR (300 MHz, CDCl<sub>3</sub>): δ 9.34 (dd, *J* = 5.4, 1.3 Hz, 1H), 8.62 (dd, *J* = 8.4, 1.3 Hz, 1H), 7.28 (dd, *J* = 8.4, 5.4 Hz, 1H), 7.12 (d, *J* = 8.6 Hz, 1H), 6.91 (d, *J* = 8.6 Hz, 1H), 3.95 (s, 3H), 3.65 (s, 6H). <sup>13</sup>C NMR (75 MHz, CDCl<sub>3</sub>): δ 160.1, 148.1, 145.6, 144.0, 134.9, 122.3, 119.8, 113.9, 108.6, 56.6, 46.3. <sup>195</sup>Pt NMR (64.5 MHz, CDCl<sub>3</sub>): δ -2764.1. HRMS (ESI): calculated for C<sub>12</sub>H<sub>14</sub>ClNO<sub>3</sub>PtSNa<sup>+</sup>, [M+Na<sup>+</sup>]<sup>+</sup> = 504.9924; found = 504.9928.

**Complex Pt4:**<sup>6,9</sup> Red solid (185.6 mg, 95 % yield). <sup>1</sup>H NMR (300 MHz, CDCl<sub>3</sub>): δ 9.36 (d, *J* = 4.0 Hz, 1H), 8.66 (d, *J* = 8.7 Hz, 1H), 7.76-7.72 (m, 1H), 7.63 (t, *J* = 7.8 Hz, 1H), 7.55-7.48 (m, 2H), 3.61 (s, 6H).

**General procedure for the synthesis of complexes [Pt5]Cl-[Pt13]Cl.** In a Schlenk flask, the corresponding complex **Pt1-Pt4** (0.2 mmol, 1.0 eq.) and phosphine ligand (0.2 mmol for bidentate phosphines or 0.4 mmol for monodentate phosphines) were added. Then, 2.0 mL of chloroform were added under nitrogen, and the reaction mixture was stirred at reflux for 24 h. Next, the solvent was removed under reduced pressure and the resultant solid was washed with cold diethyl ether and dried under vacuum.

*Complex [Pt5]Cl*: Brown solid (158.3 mg, 88% yield).  $^1\text{H}$  NMR (300 MHz,  $\text{CDCl}_3$ ):  $\delta$  8.38 (d,  $J = 8.2$  Hz, 1H), 7.63-7.32 (m, 21H), 7.32-7.26 (m, 4H), 7.24-7.15 (m, 7H), 7.08-6.97 (m, 2H), 6.46 (d,  $J = 7.8$  Hz, 1H).  $^{13}\text{C}$  NMR (75 MHz,  $\text{CDCl}_3$ ):  $\delta$  149.1, 141.7, 135.2, 135.1 (2C), 135.0, 134.9 (2C), 134.7, 134.6, 134.4, 134.3, 132.8 (2C), 132.5, 132.3 (3C), 131.1 (3C), 130.9, 129.4, 129.2, 128.9, 128.7, 128.6, 128.4, 128.2, 128.1, 128.0, 127.9, 126.6, 125.7, 121.1, 114.9, 113.2 (all the C signals are listed).  $^{31}\text{P}$  NMR (122 MHz,  $\text{CDCl}_3$ ):  $\delta$  14.1 ( $^1J_{\text{Pt,P}} = 3672.5$  Hz,  $^2J_{\text{P,P}} = 25.0$  Hz), 8.7 ( $^1J_{\text{Pt,P}} = 3394.3$  Hz,  $^2J_{\text{P,P}} = 25.0$  Hz).  $^{195}\text{Pt}$  NMR (64.5 MHz,  $\text{CDCl}_3$ ):  $\delta$  4210.3 (dd,  $^1J_{\text{Pt,P}} = 3675.2$ , 3398.3 Hz). HRMS (ESI $^+$ ): calculated for  $\text{C}_{45}\text{H}_{36}\text{NOPt}^+$ ,  $[\text{M}]^+ = 863.1919$ ; found = 863.1916.

*Complex [Pt6]Cl*: Brown solid (213.7 mg, 99% yield).  $^1\text{H}$  NMR (300 MHz,  $\text{CDCl}_3$ ):  $\delta$  8.28 (d,  $J = 7.6$  Hz, 1H), 7.60 (t,  $J = 4.9$  Hz, 1H), 7.40-7.19 (m, 13H), 7.01-6.92 (m, 2H), 6.71 (dd,  $J = 8.8$ , 2.0 Hz, 6H), 6.63 (dd,  $J = 8.8$ , 2.0 Hz, 6H), 6.47 (d,  $J = 7.2$  Hz, 1H), 3.74 (s, 9H), 3.72 (s, 9H).  $^{13}\text{C}$  NMR (75 MHz,  $\text{CDCl}_3$ ):  $\delta$  165.4, 161.5, 161.4, 161.3 (2C), 148.0, 143.9, 140.2, 135.6, 135.5, 135.0, 134.8, 130.2, 129.9, 119.9, 118.3, 117.4, 117.2, 116.2, 115.2, 113.6, 113.4, 113.3, 113.1, 112.9, 54.7 (2C) (all the C signals are listed).  $^{31}\text{P}$  NMR (122 MHz,  $\text{CDCl}_3$ ):  $\delta$  10.7 ( $^1J_{\text{Pt,P}} = 3693.9$  Hz,  $^2J_{\text{P,P}} = 24.6$  Hz), 4.9 ( $^1J_{\text{Pt,P}} = 3423.0$  Hz,  $^2J_{\text{P,P}} = 24.6$  Hz).  $^{195}\text{Pt}$  NMR (64.5 MHz,  $\text{CDCl}_3$ ):  $\delta$  4211.0 (dd,  $^1J_{\text{Pt,P}} = 3684.6$ , 3426.2 Hz). HRMS (ESI $^+$ ): calculated for  $\text{C}_{51}\text{H}_{48}\text{NO}_7\text{P}_2\text{Pt}^+$ ,  $[\text{M}]^+ = 1043.2553$ ; found = 1043.2566.

*Complex [Pt7]Cl*: Brown solid (142.6 mg, 89% yield).  $^1\text{H}$  NMR (300 MHz,  $\text{CDCl}_3$ ):  $\delta$  8.29 (d,  $J = 8.1$  Hz, 1H), 7.84 (dd,  $J = 11.3$ , 7.8 Hz, 4H), 7.67 (dd,  $J = 11.6$ , 7.9 Hz, 4H), 7.58-7.33 (m, 14H), 6.98 (d,  $J = 7.8$  Hz, 2H), 6.62 (d,  $J = 7.8$  Hz, 1H), 3.01-2.71 (m, 2H), 2.43 (s, 2H), 2.21-1.85 (m, 4H).  $^{13}\text{C}$  NMR (75 MHz,  $\text{CDCl}_3$ ):  $\delta$  166.5, 148.2, 144.4, 141.0, 133.9, 133.8, 133.6, 133.5, 133.4, 132.8, 132.1, 131.2, 131.1, 131.0, 129.9, 129.8, 128.9, 128.7, 128.4, 128.3 (2C), 128.1,

127.7, 127.6, 127.2, 126.8, 120.7, 116.3, 114.3, 28.2, 27.7, 26.2, 25.7, 23.3, 22.5 (all the C signals are listed).  $^{31}\text{P}$  NMR (122 MHz,  $\text{CDCl}_3$ ):  $\delta$  9.5 ( $^1J_{\text{Pt,P}} = 3432.9$  Hz,  $^2J_{\text{P,P}} = 29.0$  Hz), 4.2 ( $^1J_{\text{Pt,P}} = 3315.7$  Hz,  $^2J_{\text{P,P}} = 29.0$  Hz).  $^{195}\text{Pt}$  NMR (64.5 MHz,  $\text{CDCl}_3$ ):  $\delta$  -4264.4 (t,  $^1J_{\text{Pt,P}} = 3392.1$  Hz). HRMS ( $\text{ESI}^+$ ): calculated for  $\text{C}_{37}\text{H}_{34}\text{NOP}_2\text{Pt}^+$ ,  $[\text{M}]^+ = 765.1762$ ; found = 765.1760.

**Complex [Pt8]Cl:** Yellow solid (173.5 mg, 95% yield).  $^1\text{H}$  NMR (300 MHz,  $\text{CDCl}_3$ ):  $\delta$  8.39 (d,  $J = 8.1$  Hz, 1H), 8.14 (s, 2H), 7.86-6.97 (m, 27H), 6.60 (dd,  $J = 16.4, 8.1$  Hz, 3H), 6.19-6.02 (m, 1H).  $^{13}\text{C}$  NMR (75 MHz,  $\text{CDCl}_3$ ):  $\delta$  166.0, 159.1, 159.0, 158.9, 158.8, 149.3 (2C), 141.7, 137.9 (2C), 135.2, 135.0, 134.8, 134.5, 132.8 (2C), 131.9, 131.2, 131.1, 129.6, 126.4, 126.3, 125.4, 125.3, 125.1, 125.0, 121.1, 121.0, 120.9, 119.2, 119.1, 116.2, 116.1, 114.7 (all the C signals are listed).  $^{31}\text{P}$  NMR (122 MHz,  $\text{CDCl}_3$ ):  $\delta$  2.5 ( $^1J_{\text{Pt,P}} = 3553.1$  Hz,  $^2J_{\text{P,P}} = 24.3$  Hz), -1.3 ( $^1J_{\text{Pt,P}} = 3716.6$  Hz,  $^2J_{\text{P,P}} = 24.3$  Hz).  $^{195}\text{Pt}$  NMR (64.5 MHz,  $\text{CDCl}_3$ ):  $\delta$  -4154.0 (dd,  $^1J_{\text{Pt,P}} = 3709.4, 3560.7$  Hz). HRMS ( $\text{ESI}^+$ ): calculated for  $\text{C}_{45}\text{H}_{34}\text{NO}_2\text{P}_2\text{Pt}^+$ ,  $[\text{M}]^+ = 877.1711$ ; found = 877.1684.

**Complex [Pt9]Cl:** Yellow solid (193.5 mg, 97% yield).  $^1\text{H}$  NMR (300 MHz,  $\text{CDCl}_3$ ):  $\delta$  8.55-8.15 (m, 2H), 7.93-7.71 (m, 3H), 7.70-7.52 (m, 8H), 7.51-7.29 (m, 10H), 7.27-7.07 (m, 6H), 7.04 (d,  $J = 7.9$  Hz, 1H), 7.00-6.89 (m, 3H), 6.85-6.69 (m, 4H), 6.64 (d,  $J = 7.9$  Hz, 1H).  $^{13}\text{C}$  NMR (75 MHz,  $\text{CDCl}_3$ ):  $\delta$  148.5, 141.1, 137.2, 135.6, 135.5, 135.4, 135.3, 134.4 (2C), 134.3 (2C), 133.9, 133.4, 133.3, 133.2 (2C), 131.9 (2C), 131.4 (2C), 131.3, 131.2, 130.3, 130.2, 130.1, 130.0, 128.8, 128.6, 128.4, 128.3 (2C), 128.2, 127.9, 127.8, 127.7 (2C), 127.6, 127.5, 127.4 (2C), 127.2 (3C), 127.1, 125.5 (2C), 123.9 (2C), 121.2 (2C), 121.0 (2C), 120.4, 116.3, 114.5 (all the C signals are listed).  $^{31}\text{P}$  NMR (122 MHz,  $\text{CDCl}_3$ ):  $\delta$  6.5 ( $^2J_{\text{P,P}} = 29.9$  Hz), 5.1 ( $^2J_{\text{P,P}} = 29.9$  Hz).  $^{195}\text{Pt}$  NMR (64.5 MHz,  $\text{CDCl}_3$ ):  $\delta$  -4035.2 (dd,  $^1J_{\text{Pt,P}} = 3568.1, 3418.9$  Hz). HRMS ( $\text{ESI}^+$ ): calculated for  $\text{C}_{53}\text{H}_{38}\text{NOP}_2\text{Pt}^+$ ,  $[\text{M}]^+ = 961.2076$ ; found = 961.2057.

**Complex [Pt10]Cl:** Brown solid (195.1 mg, 99% yield).  $^1\text{H}$  NMR (300 MHz,  $\text{CDCl}_3$ ):  $\delta$  8.28 (d,  $J = 7.7$  Hz, 1H), 8.20-8.05 (m, 1H), 7.91-7.66 (m, 3H), 7.60-7.45 (m, 8H), 7.44-7.33 (m, 8H), 7.30-7.24 (m, 2H), 7.00 (d,  $J = 8.0$  Hz, 1H), 6.91 (dd,  $J = 8.1, 5.3$  Hz, 1H), 6.59 (d,  $J = 7.8$  Hz, 1H), 6.53 (dd,  $J = 12.8, 8.3$  Hz, 1H), 6.40 (dd,  $J = 8.1, 1.4$  Hz, 1H), 6.36-6.24 (m, 2H), 5.91 (d,  $J = 6.5$  Hz, 2H), 5.87 (s, 1H), 5.66 (s, 1H).  $^{13}\text{C}$  NMR (75 MHz,  $\text{CDCl}_3$ ):  $\delta$  166.6 (2C), 166.5 (2C), 151.1 (3C), 151.0, 148.5, 147.5, 147.3, 147.1, 147.0, 144.0, 141.0, 134.9, 134.8, 133.2 (2C), 133.0, 132.9, 132.7 (2C), 132.1 (2C), 131.2, 131.1, 130.1 (3C), 130.0, 129.5, 129.3, 129.1, 129.0, 128.9, 128.7, 128.6, 128.2, 128.0, 120.9, 118.5, 116.3, 116.2, 114.4, 109.0, 108.9, 108.8, 108.6, 102.7, 102.6 (all the C signals are listed).  $^{31}\text{P}$  NMR (122 MHz,  $\text{CDCl}_3$ ):  $\delta$  4.0 ( $^1J_{\text{Pt,P}} = 3561.1$  Hz,  $^2J_{\text{P,P}} = 30.4$  Hz), 3.5 ( $^1J_{\text{Pt,P}} = 3435.1$  Hz,  $^2J_{\text{P,P}} = 30.1$  Hz).  $^{195}\text{Pt}$  NMR (64.5 MHz,  $\text{CDCl}_3$ ):  $\delta$  -4089.2 (dd,  $^1J_{\text{Pt,P}} = 3582.9, 3393.6$  Hz). HRMS (ESI $^+$ ): calculated for  $\text{C}_{47}\text{H}_{34}\text{NO}_5\text{P}_2\text{Pt}^+$ ,  $[\text{M}]^+ = 949.1559$ ; found = 949.1557.

**Complex [Pt11]Cl:** Red solid (184.5 mg, 98% yield).  $^1\text{H}$  NMR (300 MHz,  $\text{CDCl}_3$ ):  $\delta$  8.39 (d,  $J = 8.3$  Hz, 1H), 8.31-7.73 (m, 5H), 7.67 (t,  $J = 7.7$  Hz, 1H), 7.62-7.33 (m, 8H), 7.34-7.08 (m, 12H), 6.98-6.84 (m, 2H), 6.64-6.48 (m, 2H), 6.05 (ddd,  $J = 11.3, 7.7, 1.4$  Hz, 1H), 2.58 (s, 6H).  $^{13}\text{C}$  NMR (75 MHz,  $\text{CDCl}_3$ ):  $\delta$  161.9, 159.2 (2C), 159.0, 158.9, 149.0 (2C), 144.7, 144.6 (2C), 138.3, 138.0 (2C), 135.3, 135.1, 134.7 (2C), 134.5 (2C), 133.9, 132.8, 129.6, 128.6 (2C), 126.9, 126.3, 126.2, 125.3 (2C), 125.2, 125.0, 121.7, 120.2, 119.4, 119.3 (2C), 119.1, 16.9 (2C) (all the C signals are listed).  $^{31}\text{P}$  NMR (122 MHz,  $\text{CDCl}_3$ ):  $\delta$  3.1 ( $^1J_{\text{Pt,P}} = 3531.1$  Hz,  $^2J_{\text{P,P}} = 24.8$  Hz), -1.3 ( $^1J_{\text{Pt,P}} = 3688.5$  Hz,  $^2J_{\text{P,P}} = 24.8$  Hz).  $^{195}\text{Pt}$  NMR (64.5 MHz,  $\text{CDCl}_3$ ):  $\delta$  -4149.2 (dd,  $^1J_{\text{Pt,P}} = 3678.1, 3552.0$  Hz). HRMS (ESI $^+$ ): calculated for  $\text{C}_{47}\text{H}_{38}\text{ClNO}_2\text{P}_2\text{Pt}^+$ ,  $[\text{M}]^+ = 905.2024$ ; found = 905.2034.

**Complex [Pt12]Cl:** Dark yellow solid (171.7 mg, 91% yield).  $^1\text{H}$  NMR (300 MHz,  $\text{CDCl}_3$ ):  $\delta$  8.65 (d,  $J = 7.7$  Hz, 1H), 8.35-7.76 (m, 4H), 7.70 (t,  $J = 7.7$  Hz, 1H), 7.65-7.27 (m, 12H), 7.25-7.01

(m, 9H), 6.93 (dd,  $J = 7.2, 5.6$  Hz, 1H), 6.83 (d,  $J = 8.6$  Hz, 1H), 6.65-6.51 (m, 2H), 6.48 (d,  $J = 8.5$  Hz, 1H), 6.10 (dd,  $J = 10.2, 7.7$  Hz, 1H), 3.88 (s, 3H).  $^{13}\text{C}$  NMR (75 MHz,  $\text{CDCl}_3$ ):  $\delta$  159.4, 159.3, 159.0 (2C), 158.8 (2C), 149.7 (2C), 145.8, 144.6, 144.5 (2C), 137.8, 136.8, 135.1, 135.0, 134.8, 134.7, 134.4 (2C), 133.7, 132.7 (2C), 131.8, 129.4, 126.3, 126.2, 125.3, 125.2, 125.0, 124.9, 122.8 (2C), 121.1 (2C), 120.2, 120.1, 119.8, 119.6, 119.5 (2C), 119.2, 119.1, 118.8, 114.4, 114.3, 108.8, 56.6 (all the C signals are listed).  $^{31}\text{P}$  NMR (122 MHz,  $\text{CDCl}_3$ ):  $\delta$  2.6 ( $^1J_{\text{Pt,P}} = 3521.0$  Hz,  $^2J_{\text{P,P}} = 24.4$  Hz), -1.2 ( $^1J_{\text{Pt,P}} = 3733.0$  Hz,  $^2J_{\text{P,P}} = 24.4$  Hz).  $^{195}\text{Pt}$  NMR (64.5 MHz,  $\text{CDCl}_3$ ):  $\delta$  -4136.4 (dd,  $^1J_{\text{Pt,P}} = 3733.2, 3521.3$  Hz). HRMS (ESI $^+$ ): calculated for  $\text{C}_{46}\text{H}_{36}\text{NO}_3\text{P}_2\text{Pt}^+$ ,  $[\text{M}]^+ = 907.1817$ ; found = 907.1829.

**Complex [Pt13]Cl:** Orange solid (153.1 mg, 97% yield).  $^1\text{H}$  NMR (300 MHz,  $\text{CDCl}_3$ ):  $\delta$  8.73-8.62 (m, 1H), 6.61-8.55 (m, 1H), 7.92-7.80 (m, 8H), 7.58-7.48 (m, 12H), 7.25-7.18 (m, 4H), 3.05-2.65 (m, 4H).  $^{13}\text{C}$  NMR (75 MHz,  $\text{CDCl}_3$ ):  $\delta$  155.0, 154.9, 150.0, 144.1, 142.8, 134.1, 134.0, 133.7, 133.5, 133.1 (2C), 132.8 (2C), 132.0, 131.6, 130.2, 130.0, 129.5, 129.3, 126.6, 126.3, 125.8, 125.6, 123.4, 122.2, 29.8, 29.7, 29.6, 29.5, 29.2 (2C), 29.0, 28.9 (all the C signals are listed).  $^{31}\text{P}$  NMR (122 MHz,  $\text{CDCl}_3$ ):  $\delta$  51.3 ( $^1J_{\text{Pt,P}} = 2864.1$  Hz,  $^2J_{\text{P,P}} = 8.9$  Hz), 36.8 ( $^1J_{\text{Pt,P}} = 3216.1$  Hz,  $^2J_{\text{P,P}} = 8.9$  Hz).  $^{195}\text{Pt}$  NMR (64.5 MHz,  $\text{CDCl}_3$ ):  $\delta$  -4569.4 (dd,  $^1J_{\text{Pt,P}} = 3232.2, 2859.1$  Hz). HRMS (ESI $^+$ ): calculated for  $\text{C}_{35}\text{H}_{30}\text{NP}_2\text{PtS}^+$ ,  $[\text{M}]^+ = 753.1220$ ; found = 753.1213.

**General procedure for the counteranion exchange.** To a round-bottom flask, the corresponding Pt complex (0.1 mmol, 1.0 eq.) and  $\text{KPF}_6$  (0.5 mmol, 5.0 eq.) were added. Then, 2.0 mL of a chloroform/water 1:1 (v/v) solvent mixture were added and the reaction mixture was stirred at rt. After 24 h, the resulting solid was filtered, washed with diethyl ether and dried under vacuum.

*Complex [Pt7]PF<sub>6</sub>*: Brown solid (86.5 mg, 95% yield). <sup>1</sup>H NMR (300 MHz, CDCl<sub>3</sub>) δ 8.27 (d, *J* = 8.2 Hz, 1H), 7.85 (dd, *J* = 11.8, 7.2 Hz, 4H), 7.70 (dd, *J* = 12.2, 7.3 Hz, 4H), 7.65-7.35 (m, 14H), 7.06-6.95 (m, 2H), 6.68 (d, *J* = 7.8 Hz, 1H), 2.90-2.63 (m, 4H), 2.19-1.88 (m, 4H). <sup>13</sup>C NMR (75 MHz, CDCl<sub>3</sub>) δ 166.5, 148.4, 144.4, 141.0, 133.8, 133.6, 133.4, 133.3, 132.9 (2C), 132.1, 132.0, 131.3, 130.9, 129.9, 129.8, 128.9, 128.7, 128.0, 127.5, 127.2, 126.7, 120.8, 116.2 (2C), 114.3, 28.1, 27.6, 26.0, 25.5, 23.2, 22.4 (all the C signals are listed). <sup>31</sup>P NMR (122 MHz, CDCl<sub>3</sub>) δ 9.12 (<sup>1</sup>*J*<sub>Pt,P</sub> = 3435.1 Hz, <sup>2</sup>*J*<sub>P,P</sub> = 29.1 Hz), 4.12 (<sup>1</sup>*J*<sub>Pt,P</sub> = 3313.2 Hz, <sup>2</sup>*J*<sub>P,P</sub> = 29.0 Hz), -144.30 (hept, <sup>1</sup>*J*<sub>P,F</sub> = 712.8 Hz). <sup>195</sup>Pt NMR (64 MHz, CDCl<sub>3</sub>) δ -4035.35 (dd, <sup>1</sup>*J*<sub>Pt,P</sub> = 3619.2, 3443.1 Hz). <sup>19</sup>F NMR (282 MHz, CDCl<sub>3</sub>) δ -73.46 (d, <sup>1</sup>*J*<sub>P,F</sub> = 712.8 Hz). HRMS (ESI<sup>+</sup>): calculated for C<sub>37</sub>H<sub>34</sub>NOP<sub>2</sub>Pt<sup>+</sup>, [M]<sup>+</sup> = 765.1762; found = 765.1762.

*Complex [Pt8]PF<sub>6</sub>*: Yellow solid (94.1 mg, 92% yield). <sup>1</sup>H NMR (300 MHz, CDCl<sub>3</sub>): δ 8.34 (d, *J* = 8.2 Hz, 1H), 8.30-7.69 (m, 6H), 7.70-7.08 (m, 20H), 7.10-6.92 (m, 3H), 6.81-6.50 (m, 3H), 6.14 (dd, *J* = 11.5, 7.7 Hz, 1H). <sup>13</sup>C NMR (75 MHz, CDCl<sub>3</sub>): δ 166.3, 166.2 (2C), 159.2 (2C), 159.0 (2C), 150.8, 149.5 (2C), 145.1 (2C), 141.6, 138.0, 137.9, 135.3, 135.2, 134.9 (2C), 134.7 (2C), 132.9 (2C), 132.1, 132.0, 131.3, 131.2, 129.9, 129.8, 129.7, 126.5, 126.4, 125.5, 125.4, 125.3, 125.2, 121.0 (2C), 120.9, 120.4, 119.7, 119.4, 119.3, 118.9, 116.3, 116.2, 114.8 (all the C signals are listed). <sup>31</sup>P NMR (122 MHz, CDCl<sub>3</sub>): δ 2.5 (<sup>1</sup>*J*<sub>Pt,P</sub> = 3556.2 Hz, <sup>2</sup>*J*<sub>P,P</sub> = 24.3 Hz), -1.3 (<sup>1</sup>*J*<sub>Pt,P</sub> = 3720.7 Hz, <sup>2</sup>*J*<sub>P,P</sub> = 24.3 Hz), -144.3 (hept, <sup>1</sup>*J*<sub>P,F</sub> = 712.5 Hz). <sup>19</sup>F NMR (282 MHz, CDCl<sub>3</sub>): δ -73.8 (<sup>1</sup>*J*<sub>F,P</sub> = 712.5 Hz). <sup>195</sup>Pt NMR (64.5 MHz, CDCl<sub>3</sub>): δ -4154.6 (dd, <sup>1</sup>*J*<sub>Pt,P</sub> = 3700.0, 3547.9 Hz). HRMS (ESI<sup>+</sup>): calculated for C<sub>45</sub>H<sub>34</sub>NO<sub>2</sub>P<sub>2</sub>Pt<sup>+</sup>, [M]<sup>+</sup> = 877.1711; found = 877.1677.

*Complex [Pt9]PF<sub>6</sub>*: Yellow solid (99.6 mg, 90% yield). <sup>1</sup>H NMR (300 MHz, CDCl<sub>3</sub>) δ 8.39 (s, 1H), 8.26 (d, *J* = 8.3 Hz, 1H), 7.80 (dd, *J* = 12.0, 7.8 Hz, 2H), 7.72-7.12 (m, 24H), 7.11-6.72 (m, 9H), 6.65 (d, *J* = 7.9 Hz, 1H). <sup>13</sup>C NMR (75 MHz, CDCl<sub>3</sub>) δ 166.4, 148.4, 143.8, 140.8, 139.8,

139.6, 138.8, 135.3, 135.7, 134.3, 134.2 (2C), 134.1, 133.1, 133.0, 132.6, 132.5, 132.0 (2C), 131.7, 131.3, 131.2, 131.1, 131.0, 130.1, 130.0, 129.9, 128.6, 128.4, 128.3, 128.1, 128.0, 127.9, 127.6, 127.5, 127.3, 127.1, 126.9, 126.1, 125.8, 125.6, 125.3, 124.8, 124.7, 123.8, 122.9, 121.0, 120.9, 120.7, 120.1 (2C), 116.1, 116.0, 114.3 (all the C signals are listed).  $^{31}\text{P}$  NMR (122 MHz,  $\text{CDCl}_3$ )  $\delta$  6.29 ( $^1J_{\text{Pt,P}} = 3583.2$  Hz,  $^2J_{\text{P,P}} = 29.8$  Hz), 5.21 ( $^1J_{\text{Pt,P}} = 3414.4$  Hz,  $^2J_{\text{P,P}} = 29.7$  Hz), -144.29 (hept,  $^1J_{\text{P,F}} = 712.5$  Hz).  $^{19}\text{F}$  NMR (282 MHz,  $\text{CDCl}_3$ )  $\delta$  -73.7 (d,  $^1J_{\text{F,P}} = 712.5$  Hz).  $^{195}\text{Pt}$  NMR (64 MHz,  $\text{CDCl}_3$ )  $\delta$  -4035.4 (dd,  $^1J_{\text{Pt,P}} = 3608.0$ , 3448.9 Hz). HRMS (ESI $^+$ ): calculated for  $\text{C}_{53}\text{H}_{38}\text{NOPt}^+$ ,  $[\text{M}]^+ = 961.2076$ ; found = 961.2040.

**General procedure for the oxidation of sulfides (1a-g):** A glass vial was charged with the corresponding sulfide (0.2 mmol) and corresponding platinum(II) complex (0.004 mmol, 2 mol%). Then, 2.0 mL of water were added to the vial and the reaction mixture was stirred open to the air and irradiated using a blue LEDs system (see S.I) at rt for 48 h. The crude reaction mixture was extracted with dichloromethane (2 x 5 mL) and the combined organic layers was washed with a saturated aqueous solution of  $\text{NaHCO}_3$  (2 x 5 mL), dried over  $\text{MgSO}_4$ , filtered and concentrated under reduced pressure. The obtained crude was purified by flash chromatography on silica gel to afford the final sulfoxide.

*Methyl(4-methylphenyl)sulphoxide (2a):*<sup>6a</sup> The crude mixture was purified by flash chromatography (cyclohexane / ethyl acetate 1:1 as eluent) to afford **2a** as a colourless oil (29.9 mg, 97% yield).  $^1\text{H}$  NMR (300 MHz,  $\text{CDCl}_3$ )  $\delta$  7.51 (d,  $J = 8.3$  Hz, 2H), 7.30 (d,  $J = 8.3$  Hz, 2H), 2.67 (s, 3H), 2.38 (s, 3H).

*(4-Methoxyphenyl)methylsulphoxide (2b):*<sup>6a</sup> The crude mixture was purified by flash chromatography (cyclohexane / ethyl acetate 1:1 as eluent) to afford **2b** as a yellow oil (32.3 mg,

95% yield).  $^1\text{H}$  NMR (300 MHz,  $\text{CDCl}_3$ )  $\delta$  7.58 (d,  $J$  = 8.9 Hz, 2H), 7.02 (d,  $J$  = 8.9 Hz, 2H), 3.84 (s, 3H), 2.69 (s, 3H).

*Cyclopropylphenylsulphoxide (2c)*:<sup>6a</sup> The crude mixture was purified by flash chromatography (cyclohexane / ethyl acetate 1:1 as eluent) to afford **2c** as a colourless oil (15.9 mg, 48% yield).  $^1\text{H}$  NMR (300 MHz,  $\text{CDCl}_3$ )  $\delta$  7.71-7.62 (m, 2H), 7.59-7.48 (m, 3H), 2.30-2.18 (m, 1H), 1.27-1.19 (m, 1H), 1.08-0.89 (m, 3H).

*Dibutylsulphoxide (2d)*:<sup>6a</sup> The crude mixture was purified by flash chromatography (cyclohexane / ethyl acetate 1:1 as eluent) to afford **2d** as a colourless oil (15.9 mg, 48% yield).  $^1\text{H}$  NMR (300 MHz,  $\text{CDCl}_3$ )  $\delta$  2.75-2.55 (m, 4H), 1.85-1.65 (m, 4H), 1.63-1.32 (m, 4H), 0.97 (t, 6H).

*(tert-Butyl)methylsulphoxide (2d)*:<sup>6a</sup> The crude mixture was purified by flash chromatography (cyclohexane / ethyl acetate 1:1 as eluent) to afford **2d** as a colourless oil (15.9 mg, 48% yield).  $^1\text{H}$  NMR (300 MHz,  $\text{CDCl}_3$ )  $\delta$  2.36 (s, 3H), 1.24 (s, 9H).

*L-Methionine sulphoxide (2e)*:<sup>6a</sup> **2e** was obtained pure without flash chromatography as a diastereoisomer mixture 1:1, which are epimers at sulfur (32.9 mg, 100% yield).  $^1\text{H}$  NMR (300 MHz,  $\text{D}_2\text{O}$ )  $\delta$  3.95-3.84 (m, 1H), 3.21-2.88 (m, 2H), 2.76 (s, 3H), 2.40-2.25 (m, 2H).

**Solubility determination.** The solubility of the complexes was performed in  $\text{CH}_2\text{Cl}_2$  and  $\text{H}_2\text{O}$  and determined by UV-Vis spectroscopy.<sup>20</sup> First, a four-point standard curve (absorbance vs concentration) for each complex was performed using known concentrations of complex dissolved in  $\text{CH}_2\text{Cl}_2$  or  $\text{H}_2\text{O}$ . Next, an oversaturated suspension of the complex was prepared and stirred at room temperature for 5 min. An aliquot (50-100  $\mu\text{L}$ ) of the solution was removed, diluted to a concentration within the range of the standard curve and the UV-Vis spectrum was register. The

**Comentado [SCH1]:** decidir cual de los dos meter

**Comentado [SCH2]:** si tienes una mezcla 1:1 debería de haber dos juegos de señales y habría que poner los dos, no?



solubility was calculated from the absorbance at the maximum of the MLCT band of the complex as compared with the standard curve.

#### ASSOCIATED CONTENT

**Supporting Information.** General information, materials and methods, NMR spectra and luminescence experiments, electrochemical measurements and X-ray diffraction summary data.

#### AUTHOR INFORMATION

##### Corresponding Author

\* E-mail: [silvia.cabrera@uam.es](mailto:silvia.cabrera@uam.es); [jose.aleman@uam.es](mailto:jose.aleman@uam.es)

##### Author Contributions

The manuscript was written through contributions of all authors. All authors have given approval to the final version of the manuscript.

#### ACKNOWLEDGMENT

We are grateful to the Spanish Government (RTI2018-095038-B-I00), ‘Comunidad de Madrid’ and European Structural Funds (S2018/NMT-4367) for financial support. L.M. wishes to thank CAM for the ‘Atracción de Talento’ contract. and the UAM and CAM (SI1/PJI/2019-00237)

#### ABBREVIATIONS

BINAP, 2,2'-bis(diphenylphosphino)-1,1'-binaphthyl; DPEphos, bis[(2-diphenylphosphino)phenyl]ether; dppb, bis(diphenylphosphinobutane); dppe, diphenylphosphinoethate; SEGPHOS, (4,4'-bi-benzodioxole)-5,5'-diylidiphosphine.

#### REFERENCES

1 (a) Hou, S.; Carrol, J.; Vezzu, D. A. K. Design, Synthesis and Applications of Highly Phosphorescent Cyclometalated Platinum Complexes. *Asian J. Org. Chem.* **2015**, *4*, 1210-1245.

(b) Wang, X.; Wang, S. Phosphorescent Pt(II) Emitters for OLEDs: From Triarylboron-Functionalized Bidentate Complexes to Compounds with Macrocyclic Chelating Ligands. *Chem. Rec.* **2019**, *19*, 1693-1709.

2 (a) Wong, K. M.-C.; Tang, W.-S.; Lu, X.-X.; Zhu, N.; Yam, V. W.-W. Functionalized Platinum(II) Terpyridyl Alkynyl Complexes as Colorimetric and Luminescence pH Sensors. *Inorg. Chem.* **2005**, *44*, 1492-1498.

(b) Chung, C. Y.-S.; Yam, V. W.-W. Induced Self-Assembly and Foerster Resonance Energy Transfer Studies of Alkynylplatinum(II) Terpyridine Complex Through Interaction With Water-Soluble Poly(phenylene ethynylene sulfonate) and the Proof-of-Principle Demonstration of this Two-Component Ensemble for Selective Label-Free Detection of Human Serum Albumin. *J. Am. Chem. Soc.* **2011**, *133*, 18775-18784. (c) Mauro, M.; Aliprandi, A.; Septiadi, D.; Kehr, N. S.; De Cola, L. When self-assembly meets biology: luminescent platinum complexes for imaging applications. *Chem. Soc. Rev.* **2014**, *43*, 4144-4166. (d) Bryant, M. J.; Skelton, J. M.; Hatcher, L. E.; Stubbs, C.; Madrid, E.; Pallipurath, A. R.; Thomas, L. H.; Woodall, C. H.; Christensen, J.; Fuertes, S.; Robinson, T. P.; Beavers, C. M.; Teat, S. J.; Warren, M. R.; Pradaux-Caggiano, F.; Walsh, A.; Marken, F.; Carbery, D. R.; Parker, S. C.; McKeown, N. B.; Malass-Evans, R.; Carta, M.; Raithby, P. R. A rapidly-reversible absorptive and emissive vapochromic Pt(II) pincer-based chemical sensor. *Nat. Commun.* **2017**, *8*, 1800.

3 (a) Fung, S. K.; Zou, T.; Cao, B.; Chen, T.; To, W.-P.; Yang, C.; Lok, C.-N.; Che, C.-M. Luminescent platinum(II) complexes with functionalized N-heterocyclic carbene or diphosphine selectively probe mismatched and abasic DNA. *Nat. Commun.* **2016**, *7*, 10655. (b) Pasha, S. S.; Das, P.; Rath, N. P.; Bandyopadhyay, D.; Jana, N. R.; Laskar, I. R. Water soluble luminescent

cyclometalated platinum(II) complex - A suitable probe for bio-imaging applications. *Inorg. Chem. Commun.* **2016**, *67*, 107-111. (c) Sinn, S.; Biedermann, F.; De Cola, L. Platinum Complex Assemblies as Luminescent Probes and Tags for Drugs and Toxins in Water. *Chem. Eur. J.* **2017**, *23*, 1965-1971. (d) Zhang, Y.; Luo, Q.; Zheng, W.; Wang, Z.; Lin, Y.; Zhang, E.; Lü, S.; Xiang, J.; Zhao, Y.; Wang, F. Luminescent cyclometallated platinum(II) complexes: highly promising EGFR/DNA probes and dual-targeting anticancer agents. *Inorg. Chem. Front.* **2018**, *5*, 413-424. (e) Zhang, K.; Yeung, M. C.-L.; Leung, S. Y.-L.; Yam, V. W.-W. Platinum(II) Probes for Sensing Polyelectrolyte Lengths and Architectures. *ACS Appl. Mater. Interfaces* **2020**, *12*, 8503-8512.

4 (a) Narayanam, J. M. R.; Stephenson, C. R. J. Visible light photoredox catalysis: applications in organic synthesis. *Chem. Soc. Rev.* **2011**, *40*, 102-113. (b) Prier, C. K.; Rankic, D. A.; MacMillan, D. W. C. Visible Light Photoredox Catalysis with Transition Metal Complexes: Applications in Organic Synthesis. *Chem. Rev.* **2013**, *113*, 5322-5363. (c) Ravelli, D.; Protti, S.; Fagnoni, M. Carbon-Carbon Bond Forming Reactions via Photogenerated Intermediates. *Chem. Rev.* **2016**, *116*, 9850-9913. (d) Strieth-Kalthoff, F.; James, M. J.; Teders, M.; Pitzer, L.; Glorius, F. Energy transfer catalysis mediated by visible light: principles, applications, directions. *Chem. Soc. Rev.* **2018**, *47*, 7190-7202. (e) Glaser, F.; Wenger, O. S. Recent progress in the development of transition-metal based photoredox catalysts. *Coord. Chem. Rev.* **2020**, *405*, 213129.

5 (a) Zhong, J.-J.; Meng, Q.-Y.; Wang, G.-X.; Liu, Q.; Chen, B.; Feng, K.; Tung, C.-H.; Wu, L.-Z. A Highly Efficient and Selective Aerobic Cross-Dehydrogenative-Coupling Reaction Photocatalyzed by a Platinum(II) Terpyridyl Complex. *Chem. Eur. J.* **2013**, *19*, 6443-6450. (b) Choi, W. J.; Choi, S.; Ohkubo, K.; Fukuzumi, S.; Cho, E. J.; You, Y. Mechanisms and applications of cyclometalated Pt(II) complexes in photoredox catalytic trifluoromethylation. *Chem. Sci.* **2015**, *6*, 1454-1464. (c) Chow, P.-K.; Cheng, G.; Tong, G. S. M.; To, W.-P.; Kwong, W.-L.; Low, K.-

H.; Kwok, C.-C.; Ma, C.; Che, C.-M. Luminescent Pincer Platinum(II) Complexes with Emission Quantum Yields up to Almost Unity: Photophysics, Photoreductive C-C Bond Formation, and Materials Applications. *Angew. Chem. Int. Ed.* **2015**, *54*, 2084-2089. (d) Shelar, D. P.; Li, T.-T.; Chen, Y.; Fu, W.-F. Platinum(II) Schiff Base Complexes as Photocatalysts for Visible-Light-Induced Cross-Dehydrogenative Coupling Reactions. *ChemPlusChem* **2015**, *80*, 1541-1546. (e) Zhong, J.-J.; Yang, C.; Chang, X.-Y.; Zou, C.; Lu, W.; Che, C.-M. Platinum(II) photo-catalysis for highly selective difluoroalkylation reactions. *Chem. Commun.* **2017**, *53*, 8948-8951. (f) Li, K.; Wan, Q.; Yang, C.; Chang, X.-Y.; Low, K.-H.; Che, C.-M. Air-Stable Blue Phosphorescent Tetradentate Platinum(II) Complexes as Strong Photo-Reductant. *Angew. Chem. Int. Ed.* **2018**, *57*, 14129-14133. (g) Ranieri, A. M.; Burt, L. K.; Stagni, S.; Zacchini, S.; Skelton, B. W.; Ogden, M. I.; Bissember, A. C.; Massi, M. Anionic Cyclometalated Platinum(II) Tetrazolato Complexes as Viable Photoredox Catalysts. *Organometallics* **2019**, *38*, 1108-1117.

6 (a) Casado-Sánchez, A.; Gómez-Ballesteros, R.; Tato, F.; Soriano, F. J.; Pascual-Coca, G.; Cabrera, S.; Alemán, J. Pt(II) coordination complexes as visible light photocatalysts for the oxidation of sulfides using batch and flow processes. *Chem. Commun.* **2016**, *52*, 9137-9140. (b) Casado-Sánchez, A.; Uygur, M.; González-Muñoz, D.; Aguilar-Galindo, F.; Nova-Fernández, J. L.; Arranz-Plaza, J.; Díaz-Tendero, S.; Cabrera, S.; García-Mancheño, O.; Alemán, J. 8-Mercaptoquinoline as a Ligand for Enhancing the Photocatalytic Activity of Pt(II) Coordination Complexes: Reactions and Mechanistic Insights. *J. Org. Chem.* **2019**, *84*, 6437-6447.

7 (a) Ballardini, R.; Indelli, M. T.; Varani, G.; Bignozzi, C. A.; Scandola, F. Bis(8-quinolinolato)platinum(II): a Novel Complex Exhibiting Efficient, Long-Lived Luminescence in Fluid Solution. *Inorg. Chim. Acta* **1978**, *31*, 423-424. (b) Ballardini, R.; Varani, G.; Indelli, M. T.; Scandola, F. Phosphorescent 8-Quinolinol Metal Chelates. Excited-State Properties and Redox

Behavior. *Inorg. Chem.* **1986**, *25*, 3858-3865. (c) Shavaleev, N. M.; Adams, H.; Best, J.; Edge, R.; Navaratnam, S.; Weinstein, J. A. Deep-Red Luminescence and Efficient Singlet Oxygen Generation by Cyclometalated Platinum(II) Complexes with 8-Hydroxyquinolines and Quinoline-8-thiol. *Inorg. Chem.* **2006**, *45*, 9410-9415.

8 For other luminescent 8-quinolate complexes see for example: (a) Kunkely, H.; Vogler, A. Photoluminescence of 8-quinolinato(tetracarbonyl)rhenium(I). *Inorg. Chem. Commun.* **1998**, 398-401. (b) Warren, J. T.; Chen, W.; Johnston, D. H.; Turro, C. Ground-State Properties and Excited-State Reactivity of 8-Quinolate Complexes of Ruthenium(II). *Inorg. Chem.* **1999**, *38*, 6187-6192. (c) Kunkely, H.; Vogler, A. Optical properties of zinc(II) 5,7-diiodo-8-quinolinolate in solution. Phosphorescence under ambient conditions. *Chem. Phys. Lett.* **2003**, *376*, 226-229. (d) Yue, C.; Jiang, F.; Xu, Y.; Yuan, D.; Chen, L.; Yan, C.; Hong, M. The Aggregations and Strong Emissions of  $d^8$  and  $d^{10}$  Metal-8-Hydroxyquinoline Complexes. *Cryst. Growth Des.* **2008**, *8*, 2721-2728. (e) Bellinger-Buckley, S.; Chang, T.-C.; Bag, S.; Schweinfurth, D.; Zhou, W.; Torok, B.; Sarkar, B.; Tsai, M.-K.; Rochford, J. Exploring the Noninnocent Character of Electron Rich  $\pi$ -Extended 8-Oxyquinolate Ligands in Ruthenium(II) Bipyridyl Complexes. *Inorg. Chem.* **2014**, *53*, 5556-5567; (f) Shahedi, Z.; Jafari, M. R.; Zolanvari, A. A. Synthesis of  $ZnQ_2$ ,  $CaQ_2$ , and  $CdQ_2$  for application in OLED: optical, thermal, and electrical characterizations. *J. Mater. Sci.: Mater. Electron.* **2017**, *28*, 7313-7319.

9 Martín Santos, C.; Cabrera, S.; Padrón, J.; López Solera, I.; Quiroga, A.; Medrano, M. A.; Navarro-Ranninger, C.; Alemán, J. Novel clinoquinol and its analogous platinum complexes: importance, role of the halogen substitution and the hydroxyl group of the ligand. *Dalton Trans.* **2013**, *42*, 13343-13348.

10 (a) Sakaki, S.; Hashimoto, S.; Koga, G.; Ohkubo, K. Significant Phosphine Ligand Effect on the Photochemical Reactivity of  $[\text{Cu}(\text{N-N})\text{L}_2]^+$  (N-N = 1,10-phenanthroline or 2,9-dimethyl-1,10-phenanthroline; L = tertiary phosphine). *J. Chem. Soc. Dalton Trans.* **1988**, 1641-1644. (b) Sakaki, S.; Mizutano, H.; Kase, Y.; Inokuchi, K.; Arai, T.; Hamada, T. Photoinduced electron transfer between  $[\text{Cu}(\text{dmphen})\text{L}_2]^+$  [dmphen = 2,9-dimethyl-1,10-phenanthroline, L =  $\text{PPh}_n(\text{C}_6\text{H}_4\text{OMe-}p)_3$ ,  $n$  (n = 0-3)] and methyl viologen. *J. Chem. Soc. Dalton Trans.* **1996**, 1909-1914. (c) Cuttell, D. G.; Kuang, S. M.; Fanwick, P. E.; McMillin, D. R.; Walton, R. A. Simple Cu(I) Complexes with Unprecedented Excited-State Lifetimes. *J. Am. Chem. Soc.* **2002**, *124*, 6-7. (d) Starosta, R.; Puchalska, M.; Cybinska, J.; Barys, M.; Mudring, A. V. Structures, electronic properties and solid state luminescence of Cu(I) iodide complexes with 2,9-dimethyl-1,10-phenanthroline and aliphatic aminomethylphosphines or triphenylphosphine. *Dalton Trans.* **2011**, *40*, 2459-2468. (e) Moussa, J.; Chaminel, T.; Freeman, G. R.; Chamoreau, L. M.; Williams, J. A. G.; Amouri, H. An unprecedented cyclometallated platinum(II) complex incorporating a phosphinine co-ligand: synthesis and photoluminescence behavior. *Dalton Trans.* **2014**, *43*, 8162-8165. (f) Wang, B.; Shelar, D. P.; Han, X. Z.; Li, T. T.; Guan, X.; Lu, W.; Liu, K.; Chen, Y.; Fu, W. F.; Che, C. M. Long-Lived Excited States of Zwitterionic Copper(I) Complexes for Photoinduced Cross-Dehydrogenative Coupling Reactions. *Chem. Eur. J.* **2015**, *21*, 1184-1190. (g) Aghakhanpour, R. B.; Nabavizadeh, S. M.; Rashidi, M.; Kubicki, M. Luminescence properties of some monomeric and dimeric cycloplatinated(II) complexes containing biphosphine ligands. *Dalton Trans.* **2015**, *44*, 15829-15842. (h) Shahsavari, H. R.; Aghakhanpour, R. B.; Nikraves, M.; Ozdemir, J.; Haghighi, M. G.; Notash, B.; Beyzari, M. H. Highly Emissive Cycloplatinated(II) Complexes Obtained by the Chloride Abstraction from the Complex  $[\text{Pt}(\text{ppy})(\text{PPh}_3)(\text{Cl})]$ : Employing Various Silver Salts. *Organomet.* **2018**, *37*, 2890-2900. (i) Zhang, Y.; Schulz, M.; Wächter, M.; Karnahl,

M.; Dietzek, B. Heteroleptic diimine–diphosphine Cu(I) complexes as an alternative towards noble-metal based photosensitizers: Design strategies, photophysical properties and perspective applications. *Coord. Chem. Rev.* **2018**, *356*, 127-146.

11 Henderson, W.; Oliver, A. G. Further studies on the coordination chemistry of [Pt<sub>2</sub>(μ-S)<sub>2</sub>(PPh<sub>3</sub>)<sub>4</sub>] towards indium(III) substrates. *Inorg. Chim. Acta* **2011**, *375*, 248-255.

12 (a) Rigamonti, L.; Forni, A.; Manassero, M.; Manassero, C.; Pasini, A. Cooperation between Cis and Trans Influences in *cis*-Pt<sup>II</sup>(PPh<sub>3</sub>)<sub>2</sub> Complexes: Structural, Spectroscopic, and Computational Studies. *Inorg. Chem.* **2010**, *49*, 123; (b) Chauhan, R. S.; Kedarnath, G.; Wadawale, A.; Maity, D. K.; Jain, V. K. Cis configured bis phosphine platinum(II) chalcogenolate complexes: Structures, NMR and computational studies. *J. Organomet. Chem.* **2013**, *737*, 40; (c) W. Villarreal, L. Colina-Vegas, C. Rodrigues de Oliveira, J. C. Tenorio, J. Ellena, F. C. Gozzo, M. R. Cominetti, A. G. Ferreira, M. A. Barbosa Ferreira, M. Navarro, A. A. Batista. Chiral Platinum(II) Complexes Featuring Phosphine and Chloroquine Ligands as Cytotoxic and Monofunctional DNA-Binding Agents. *Inorg. Chem.* **2015**, *54*, 11709, (d) Shahsavari, H. R.; Fereidoonenezhad, M.; Niazi, M.; Mosavi, S. T.; Kazemi, S. H.; Kia, R.; Shirkhan, S.; Aghdama, S. A.; Raithby, P. A. Cyclometalated platinum(II) complexes of 2,2'-bipyridine *N*-oxide containing a 1,1'-bis(diphenylphosphino)ferrocene ligand: structural, computational and electrochemical studies. *Dalton Trans.* **2017**, *46*, 2013.

13 CCDC 2000822 (**Pt6**[Cl]), CCDC 2000829 (**Pt7**[PF<sub>6</sub>]), CCDC 2000838 (**Pt8**[Cl]), CCDC 2000843 (**Pt9**[PF<sub>6</sub>]) and CCDC 2000844 (**Pt13**[Cl]) contain the crystallographic data of the complexes. These data can be obtained free of charge from The Cambridge Crystallographic Data Centre via [www.ccdc.cam.ac.uk/data\\_request/cif](http://www.ccdc.cam.ac.uk/data_request/cif).

14 Adams, G. M.; Weller, A. S. POP-type ligands: Variable coordination and hemilabile behaviour. *Coord. Chem. Rev.* **2018**, 355, 150.

15 Birkholz, M.-N.; Freixa, Z.; van Leeuwen, P. W. N. M. Bite angle effects of diphosphines in C–C and C–X bond forming cross coupling reactions. *Chem. Soc. Rev.* **2009**, 38, 1099.

16 Zhou, C.-H.; Zhao, X. Theoretical investigation on quinoline-based platinum (II) complexes as efficient singlet oxygen photosensitizers in photodynamic therapy. *J. Organomet. Chem.* **2011**, 696, 3322.

17 (a) Brooks, J.; Babayan, Y.; Lamansky, S.; Djurovich, Peter I.; Tsyba, I.; Bau, R. Thompson, M. E. Synthesis and characterization of phosphorescent cyclometalated platinum complexes. *Inorg. Chem.* **2002**, 41, 3055; (b) O'Brien, C.; Wong, M. Y.; Cordes, D. B.; Slawin, A. M. Z.; Zysman-Colman, E. Cationic platinum(II) complexes bearing aryl-BIAN ligands: Synthesis and Structural and Optoelectronic Characterization, *Organometallics* **2015**, 34, 13.

18 For selected examples on photooxidations of sulfides see: (a) Zen, J.-M.; Liou, S.-L.; Kumar A. S.; Hsia, M.-S. An Efficient and Selective Photocatalytic System for the Oxidation of Sulfides to Sulfoxides. *Angew. Chem., Int. Ed.* **2003**, 42, 577-579. (b) Bonesi, S. M.; Manet, I.; Freccero, M.; Fagnoni, M.; Albini, A. Photosensitized Oxidation of Sulfides: Discriminating Between the Singlet-Oxygen Mechanism and Electron Transfer Involving Superoxide Anion or Molecular Oxygen. *Chem. Eur. J.* **2006**, 12, 4844-4857. (c) Dad'ová, J.; Svobodová, E.; Sikorski, M.; König, B.; Cibulka, R. Photooxidation of Sulfides to Sulfoxides Mediated by Tetra-O-Acetylriboflavin and Visible Light. *ChemCatChem* **2012**, 4, 620-623. (d) Gu, X.; Li, X.; Chai, Y.; Yang, Q.; Li, P.; Yao, Y. A simple metal-free catalytic sulfoxidation under visible light and air. *Green Chem.* **2013**, 15, 357-361. (e) Casado-Sánchez, A.; Gómez-Ballesteros, R.; Tato, F.; Soriano, F. J.; Pascual-



Coca, G.; Cabrera, S.; Alemán, J. Pt(II) coordination complexes as visible light photocatalysts for the oxidation of sulfides using batch and flow processes. *Chem Commun* **2016**, 52, 9137-9140. (f) Wang, H.; Wagner, G. W.; Lu, A. X.; Nguyen, D. L.; Buchanan, J. H.; McNutt, P. M.; Karwacki, C. J. Photocatalytic Oxidation of Sulfur Mustard and Its Simulant on BODIPY-Incorporated Polymer Coatings and Fabrics. *ACS Appl. Mater. Interfaces* **2018**, 10, 18771–18777. (g) Vaquero, M.; Ruiz-Riaguas, A.; Martínez-Alonso, M.; Jalón, F. A.; Manzano, B. R.; Rodríguez, A. M.; García-Herbosa, G.; Carbayo, A.; García, B.; Espino, G. Selective Photooxidation of Sulfides Catalyzed by Bis-cyclometalated Ir<sup>III</sup> Photosensitizers Bearing 2,2'-Dipyridylamine-Based Ligands. *Chem. Eur. J.* 2018, 24, 10662-10671. (h) Wei, L.-Q.; Ye, B.-H. Cyclometalated Ir-Zr Metal-Organic Frameworks as Recyclable Visible-Light Photocatalysts for Sulfide Oxidation into Sulfoxide in Water. *ACS Appl. Mater. Interfaces* **2019**, 11, 41448–41457. (i) Guo, H.; Xia, H.; Ma, X.; Chen, K.; Dang, C.; Zhao, J.; Dick, B. Efficient Photooxidation of Sulfides with Amidated Alloxazines as Heavy-atom-free Photosensitizers. *ACS Omega* **2020**, 5, 10586–10595. (j) López-Magano, A.; Platero-Prats, A. E.; Cabrera, S.; Mas-Ballesté, R.; Alemán, J. Incorporation of photocatalytic Pt(II) complexes into imine-based layered covalent organic frameworks (COFs) through monomer truncation strategy. *App. Cat. B: Environ.* **2020**, 272, 119027.

19 (a) Carreño, M. C.; Hernández-Torres, G.; Ribagorda, M.; Urbano, A. Enantiopure sulfoxides: recent applications in asymmetric synthesis. *Chem. Commun.* **2009**, 6129; (b) Feng, M.; Tang, B.; Liang, S. H.; Jiang, X. Sulfur Containing Scaffolds in Drugs: Synthesis and Application in Medicinal Chemistry. *Curr. Top. Med. Chem.* **2016**; 16, 1200.

20 Alsenz, J.; Kansy, M. High throughput solubility measurement in drug discovery and development. *Adv. Drug Deliv. Rev.* **2007**, 59, 546; (b) Pérez, C.; Díaz-García, C. V.; Agudo-López, A.; del Solar, V.; Cabrera, S.; Agulló-Ortuño, M. T.; Navarro-Ranninger, C.; Alemán, J.;

López-Martín, J. A. Evaluation of novel *trans*-sulfonamide platinum complexes against tumor cell lines. *Eur. J. Med. Chem.* **2014**, *76*, 360.

21 (a) Long, B.; Ding, Z.; Wang, X. Carbon Nitride for the Selective Oxidation of Aromatic Alcohols in Water under Visible Light. *ChemSusChem* **2013**, *6*, 2074-2078. (b) Xue, D.; Jia, Z.-H.; Zhao, C.-J.; Zhang, Y.-Y.; Wang, C.; Xiao, J. Direct Arylation of N-Heteroarenes with Aryldiazonium Salts by Photoredox Catalysis in Water. *Chem. Eur. J.* **2014**, *20*, 2960-2965. (c) Ilkaeva, M.; Krivtsov, I.; Bartashevich, Khainakov, S. A.; García, J. R.; Díaz, E.; Ordóñez, S. Carbon nitride assisted chemoselective C–H bond photo-oxidation of alkylphenolethoxylates in water medium. *Green Chem.* **2017**, *19*, 4299-4304. (d) Bu, M.-J. Cai, C.; Gallou, F.; Lipshutz, B. H. PQS-enabled visible-light iridium photoredox catalysis in water at room temperature. *Green Chem.* **2018**, *20*, 1233-1237. (e) Wang, J.; Xue, L.; Hong, M.; Ni, B.; Niu, T. Heterogeneous visible-light-induced Meerwein hydration reaction of alkenes in water using mpg-C<sub>3</sub>N<sub>4</sub> as a recyclable photocatalyst. *Green Chem.* **2020**, *22*, 411-416. (f) Biswas, S.; Kumar, M.; Levine, A. M.; Jimenez, I.; Ulijn, R. V.; Braunschweig, A. B. Visible-light photooxidation in water by <sup>1</sup>O<sub>2</sub>-generating supramolecular hydrogels. *Chem. Sci.* **2020**, *11*, 4239-4245. (g) Pfund, B.; Steffen, D. M.; Schreier, M. R.; Bertrams, M. -S.; Ye, C.; Börjesson, K.; Wenger, O. S.; Kerzig, C. UV Light Generation and Challenging Photoreactions Enabled by Upconversion in Water. *J. Am. Chem. Soc.* **2020**, *142*, 10468-10476.

21 Cini, R.; Donati, A.; Giannettoni, R. Synthesis and structural characterization of chloro(2,2';6',2''-terpyridine)platinum(II) trichloro(dimethylsulfoxide)platinate(II). Density functional analysis of model molecules. *Inorg. Chim. Acta* **2001**, *315*, 73-80.



**SYNOPSIS.** A new family of cationic Pt complexes ( $[\text{Pt}(\text{QO/S})(\text{P}^{\wedge}\text{P})]\text{X}$ ), having 8-oxy or 8-thioquinolinate (QO/S) and seven different mono or bidentate phosphines as ligands have been synthesized, characterized and studied as photocatalysts.

